AD-A129 842 ELECTRIC FIELDS IN EARTH ORBITAL SPACE(U) MCDONNELL DOUGLAS ASTRONAUTICS CO-HB HUNTINGTON BEACH CA W P OLSON ET AL. MAY 83 MDC-H0731 N00014-80-C-0796 1/1

UNCLASSIFIED F/G 4/1 NL

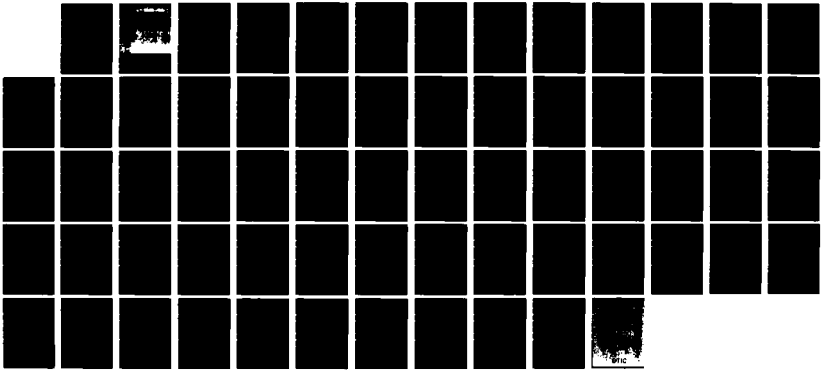

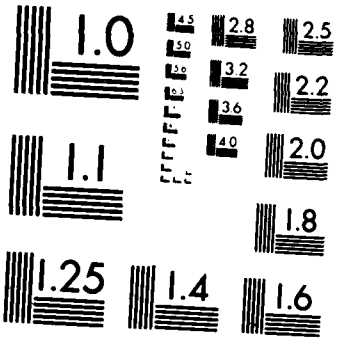

(12)

AD A129842

ELECTRIC FIELDS IN EARTH ORBITAL SPACE

ANNUAL REPORT

CONTRACT N00014-80-C-0796

MAY 1983

MDC-H0731

MCDONNELL DOUGLAS CORPORATION

ELECTRIC FIELDS IN EARTH ORBITAL SPACE

ANNUAL REPORT

CONTRACT N00014-80-C-0796

MAY 1983 MDC-H0731

by

Principal Investigator: W. P. Olson

Co-Investigator: K. A. Pfitzer

Sponsored by
Office of Naval Research
Washington, D.C. 20350

MCDONNELL DOUGLAS ASTRONAUTICS COMPANY-HUNTINGTON BEACH
5301 Bolsa Avenue Huntington Beach, California 92647 (714) 896-3311

SECURITY CLASSIFICATION OF THIS PAGE (When Data Entered)

REPORT DOCUMENTATION PAGE

READ INSTRUCTIONS BEFORE COMPLETING FORM

1. REPORT NUMBER: MDC-H0731	2. GOVT ACCESSION NO.
3. RECIPIENT'S CATALOG NUMBER	
4. TITLE (and Subtitle): ELECTRIC FIELDS IN EARTH ORBITAL SPACE ANNUAL REPORT	5. TYPE OF REPORT & PERIOD COVERED: Annual Report
6. PERFORMING ORG. REPORT NUMBER	
7. AUTHOR(s): W. P. Olson, K. A. Pfitzer	8. CONTRACT OR GRANT NUMBER(s): N00014-80-C-0796
9. PERFORMING ORGANIZATION NAME AND ADDRESS: McDonnell Douglas Astronautics Company, 5301 Bolsa Avenue, Huntington Beach, CA 92647	10. PROGRAM ELEMENT, PROJECT, TASK AREA & WORK UNIT NUMBERS: W8QA2002
11. CONTROLLING OFFICE NAME AND ADDRESS: Office of Naval Research, Washington, D.C. 20350	12. REPORT DATE: May 1983
	13. NUMBER OF PAGES
14. MONITORING AGENCY NAME & ADDRESS (if different from Controlling Office)	15. SECURITY CLASS. (of this report): Unclassified
	15a. DECLASSIFICATION/DOWNGRADING SCHEDULE

16. DISTRIBUTION STATEMENT (of this Report)

DISTRIBUTION STATEMENT A
Approved for public release;
Distribution Unlimited

17. DISTRIBUTION STATEMENT (of the abstract entered in Block 20, if different from Report)

18. SUPPLEMENTARY NOTES

19. KEY WORDS (Continue on reverse side if necessary and identify by block number)

induced electric fields, plasma sheet, plasma mantle, boundary layer
magnetosphere, magnetic fields
pressure balance
electrostatic fields

20. ABSTRACT (Continue on reverse side if necessary and identify by block number)

Work accomplished during the past year is reported. We have determined conclusively that a fraction of the magnetosheath plasma routinely has access to the magnetosphere. This entry occurs preferentially along the flanks of the tail and on the polar side of the dayside cusp regions. This entry occurs in the steady state and is responsible for the maintenance of several current state magnetic features. We have continued our involvement with the magnetospheric CDAWS, and have now constructed event models of the

-CONTINUED-

DD FORM 1 JAN 73 1473 EDITION OF 1 NOV 65 IS OBSOLETE

SECURITY CLASSIFICATION OF THIS PAGE (When Data Entered)

20. ABSTRACT

magnetic and electric fields for 3 epochs. Our magnetic field models adequately represent the magnetic field over the dayside magnetosphere. However, near midnight at geosynchronous orbit and in the near tail region, there is a large discrepancy between observation and model predictions. We believe that this is caused by the current neglect in the models of the closure of the Birkeland Region 2 currents in the vicinity of the inner edge of the plasma sheet. We have also developed procedures for the mapping of electric fields along magnetic field lines when time varying magnetic fields (and an induced component of the electric field) are present. These procedures are being tested with STARE and GEOS-2 data.

TABLE OF CONTENTS

Section 1

OVERVIEW

Work performed under Contract with ONR (N00014-80-C-0796) through the period ending in April 1983 is summarized.

In earlier work, we have developed quantitative models of the magnetic field associated with the three major magnetospheric current systems; the magnetopause, ring and tail currents. Since our goal is to quantitatively understand and model magnetospheric processes, it has been also necessary for us to understand and model quantitatively the magnetospheric electric field. Our quantitative work on the magnetospheric magnetic field put us in a position to describe and model the induced electric field associated with time variations in the magnetic field. However, since the magnetosphere is filled with plasma, the total electric field formed in response to changes in the magnetic field is somewhat different than just the induced electric field. The plasma response to the presence of the induced electric field causes additional electrostatic fields to form. We have developed procedures for determining the total electric field associated with time variations in the magnetic field.

However, it is known from the study of motions of low energy plasmas in the magnetosphere that electrostatic fields are present at all times in the tail of the magnetoshere, and also in the polar region. This led us to also understand the formation and maintenance of these electrostatic fields. It was our feeling that by describing these electrostatic fields we would have a basis for modeling both the magnetospheric magnetic and electric fields. Our

attempts at understanding the source of the electrostatic field led us to consider in more detail the classical pressure balance formalism and the assumption of specular reflection of charged particles off of the geomagnetic field. We have found that in a realistic magnetospheric magnetic field geometry, some of the low energy (1 keV) particles from the magnetosheath can gain permanent access to the magnetosphere. This entry process has now been studied in some detail and, we believe, is the explanation for the electrostatic fields that persist across the tail of the magnetosphere and over the polar cap regions. It also explains the existence of several other steady state magnetospheric features.

We have continued our work on understanding and modeling time variations in the magnetospheric magnetic field. We have now developed models for three magnetospheric events, where the magnetic field changes abruptly and continually over a period of time. These events have been studied with many other investigators as part of the CDAW (Coordinated Data Analysis Workshop) process. We have recently found that the extension of the Birkeland Region 2 currents into the magnetosphere is an important contributor to the magnetic field in the near tail region, and must be added to our quantitative magnetic field model.

The remainder of this report is divided into four sections. In the first, the entry of charged particles into the magnetosphere is discussed along with our qualitative picture of the effects this entry has on several steady state (or ground state) magnetospheric features. Our work during the last year on time varying magnetic fields and induced electric fields for specific magnetospheric events, performed in association with the CDAW workshops, is

reported in the section on time varying magnetic and electric fields. This is followed by a brief discussion of some procedures we have developed for the mapping of electric fields from ionospheric to satellite orbital altitudes. There are now data sets available from the STARE radar, and some satellites whose magnetic footprint resides within the STARE radar grid. Attempts have been made to compare data from the two regions, using the assumption of equipotential magnetic field lines. In our mapping procedure, we may abandon that assumption and assume that induced electric fields are present. In the final section, we list our publications and presentations that have occurred during the past year.

Section 2

THE ENTRY OF LOW ENERGY PLASMA INTO THE MAGNETOSPHERE

The transfer of energy from the solar wind to the magnetosphere has generally been suggested to occur by one of two mechanisms. Axford and Hines suggested that a viscous interaction between the magnetosphere and the solar wind occurring at the magnetopause provided energy for convection of plasma through the magnetosphere and thereby explained several magnetospheric processes. Dungey and Levy et al. suggested instead that the interconnection of the earth's magnetic field and the interplanetary field could act to transmit the solar wind electric field to the magnetosphere which again produced convection of the magnetospheric plasma. We have examined the direct entry of magnetosheath plasma into the magnetosphere, which occurs at all times and provides both energy and charged particles to the magnetosphere.

By the early 1960's it was known that the extension of the geomagnetic field, B, into space is limited by the solar wind. Basically, their interaction consists of the protons and electrons in the solar wind being deflected in opposite directions by the geomagnetic field. This motion forms the magnetopause current system whose associated magnetic field adds to the geomagnetic field within the magnetosphere and vectorially cancels it out beyond the magnetopause. The magnetopause is then found where the streaming pressure of the solar wind is equal to the pressure of the geomagnetic field (i.e., its energy density). These studies tacitly assumed that because of the large dimensions of the magnetosphere with respect to the charged particle gyroradii, all solar wind particles are reflected specularly off of the geomagnetic field, $\vec{B}$. The deflection of the charged particles by the

geomagnetic field is shown schematically in Figure 1, with the assumption of specular reflection. In a uniform magnetic field, all particles penetrate into the field region a distance less than 2 ion gyroradii and no particles permanently enter the magnetosphere.

Although these early magnetopause models assumed that the magnetosphere is closed, it was known that some solar cosmic ray particles can enter the magnetosphere. Since they sample such a large region of the magnetosphere that the uniform magnetic field assumption cannot be made in their case. That is, gradients in the magnetic field that occur over the paths these particles follow when they initially interact with the geomagnetic field permit them to "gradient drift" into the magnetosphere. It is then natural to ask what is the lowest energy particle that can gain access to the magnetosphere because of gradients in the geomagnetic field.

The motion of charged particles in the presence of a magnetic field containing a parallel gradient is illustrated schematically in Figure 2. Electron and positive ion trajectories are shown on both the dawn and dusk sides of the magnetopause. Note that unlike the examples shown in Figure 1 (where specular reflection was assumed and no particles enter), it is possible for some particles to permanently enter the magnetosphere. For entry to occur, a finite parallel gradient must be present and it must possess a component perpendicular to $\vec{B}$. The noon-midnight meridian plane is a symmetry plane over which no entry occurs because there is no parallel gradient perpendicular to $\vec{B}$.

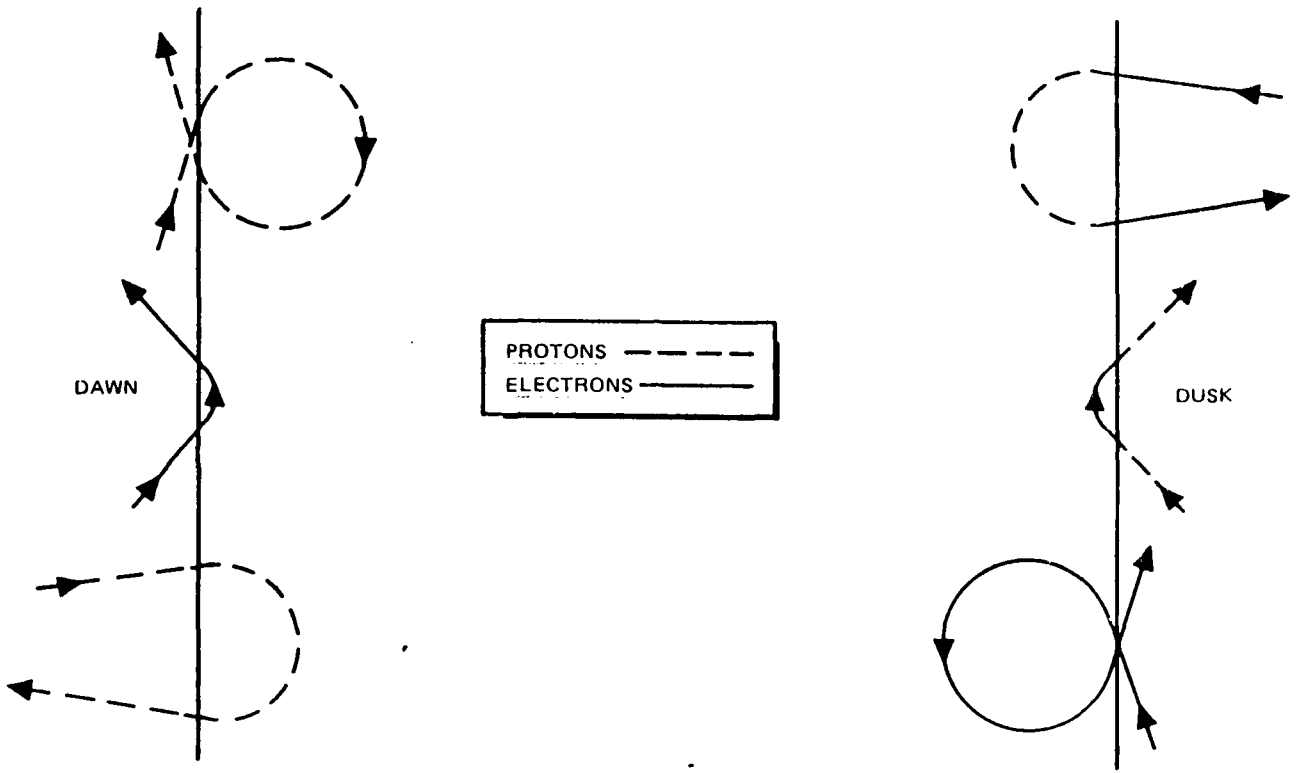

Figure 1

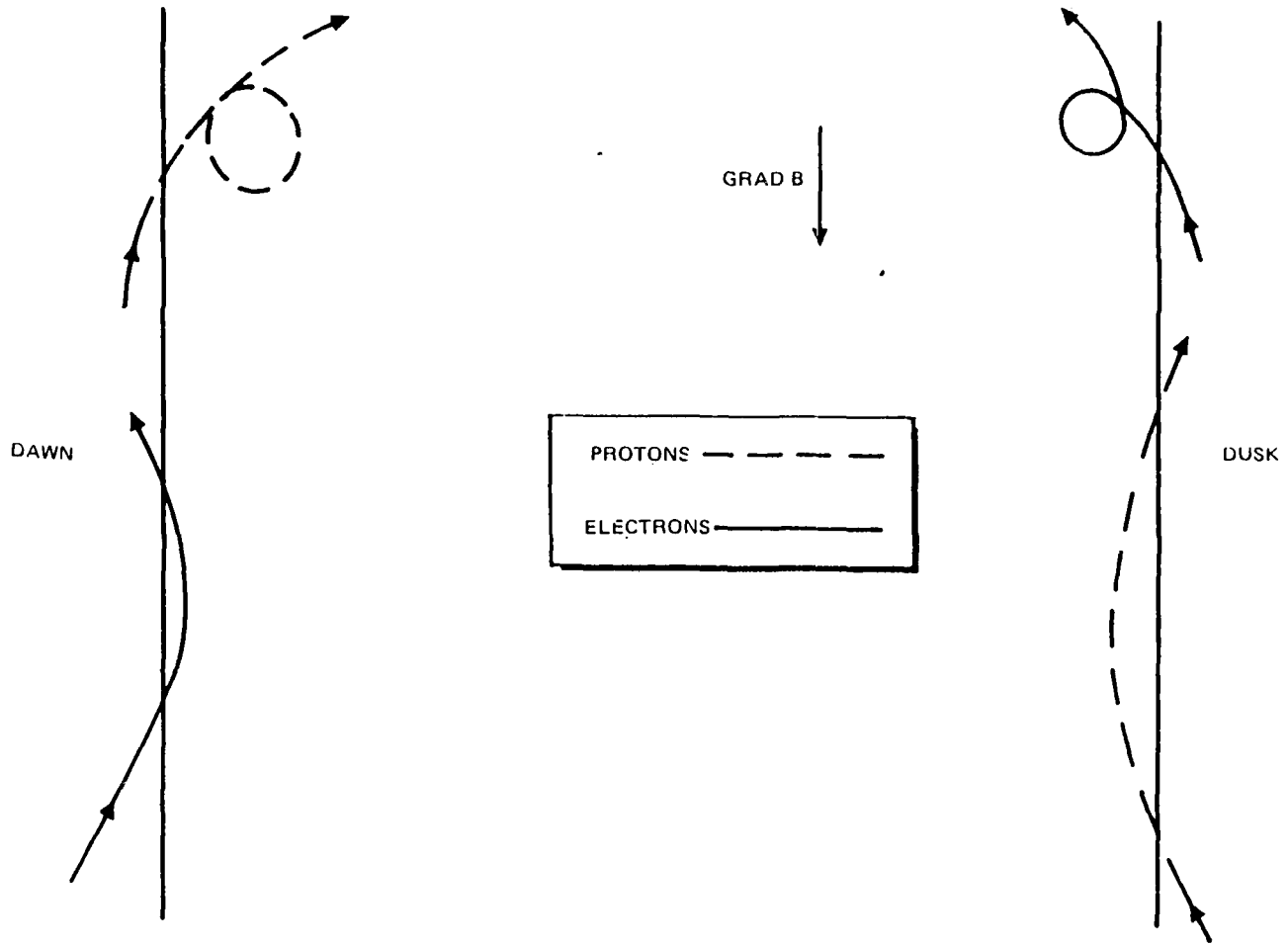

Figure 2

Particle entry into the tail of the magnetosphere in a realistic magnetic field topology was examined quantitatively assuming that the magnetic field just beyond the magnetopause is exactly zero and given by the Olson and Pfitzer (1974) model at locations within the magnetosphere. Proton "entry fractions" into this magnetically closed magnetosphere were determined using numerical techniques. Proton and electron trajectories at different locations on the magnetopause were determined by integrating the the Lorentz force equation for several particle energies and various impact angles.

The range of impact angles over which particles can gain access to the magnetosphere at a particular point on the magnetopause is illustrated in Figure 3. A polar graph is shown for the plane tangent to the magnetopause at the impact point. The projection of the solar magnetospheric x axis onto the plane is also indicated. Circles of constant elevation angle above the impact plane are shown, thus the point marked 90 degrees indicates a particle impact perpendicular to the surface. The figure suggests that at a distance of 20 R_E down the tail near the magnetic equator on the dawn side, just under 4 percent of an isotropic distribution of 1 keV protons will enter the magnetosphere. The entry fraction referred to in Figure 4 is defined as the number of entering particles divided by the total number of incident particles at a point. Several hundred trajectories were run to determine the entry fraction at each point for a particular particle energy, mass and charge. A comparison of Figures 3b and 3c illustrates that the entry fraction for protons is approximately 40 times larger than that of similar energy electrons in the same magnetic field (X, -Y, Z for protons, and X, Y, Z for electrons). The ratio of protons entering on the dawn flank to electrons entering on the dusk flank, however, is only about two to one, owing to the greater speed of the electrons.

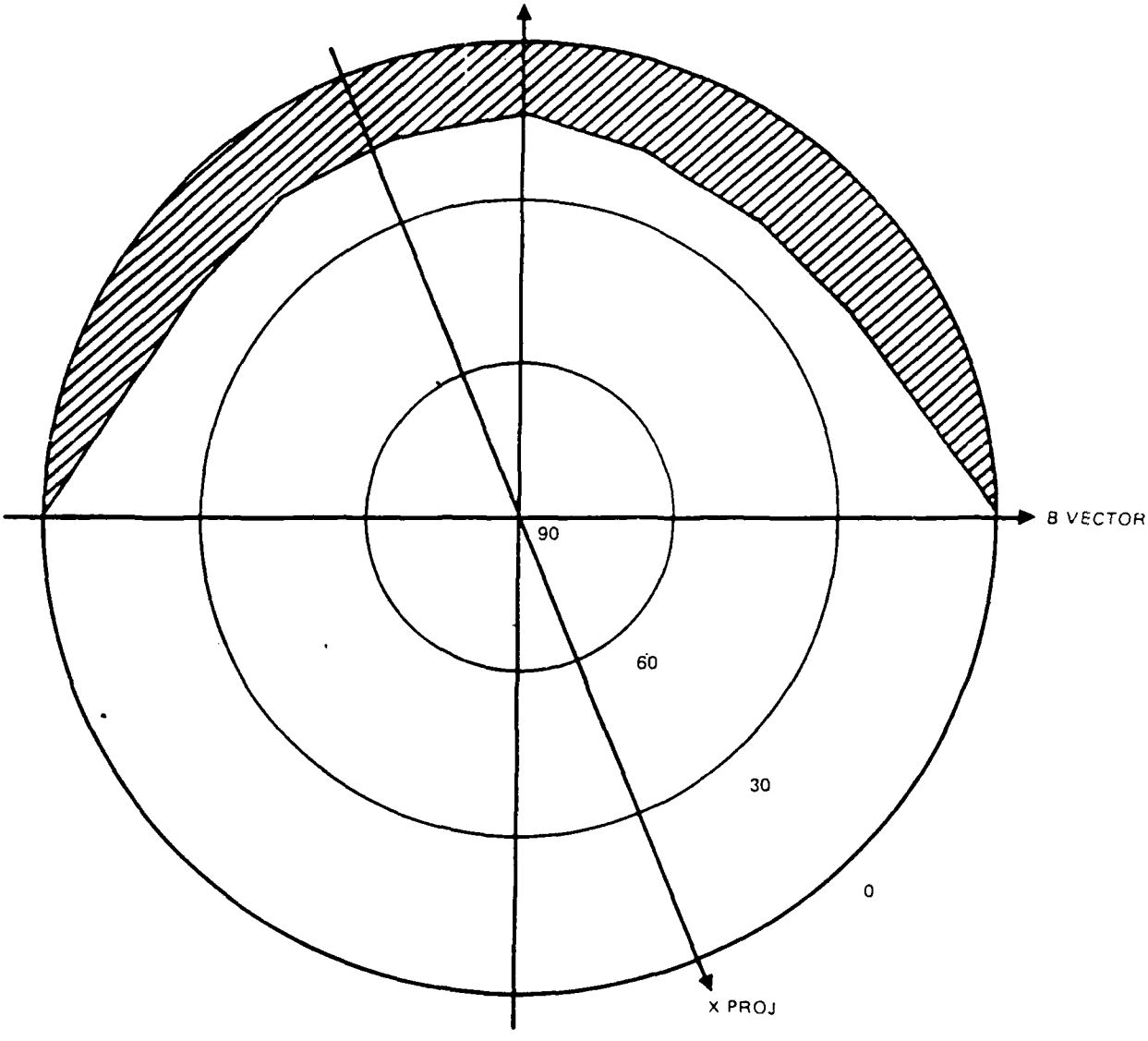

BOUNDARY POSITION -20.00 -17.90 3.16

ENERGY (KEV). 1 ENTRY FRACTION 0.0394

Figure 3a

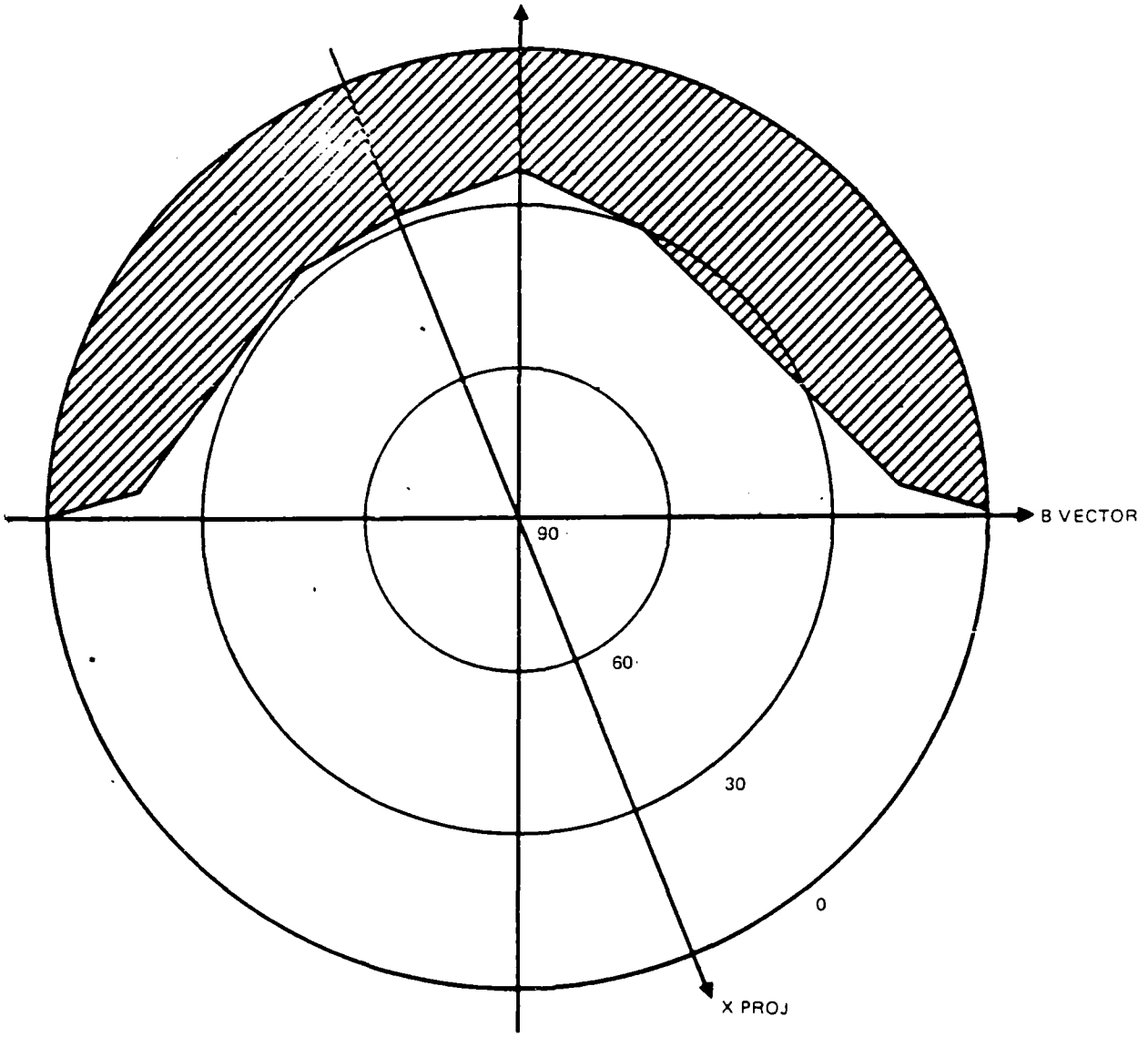

BOUNDARY POSITION: -20.00 -17.90 3.16

ENERGY (KEV): 10 ENTRY FRACTION: 0.1054

Figure 3b

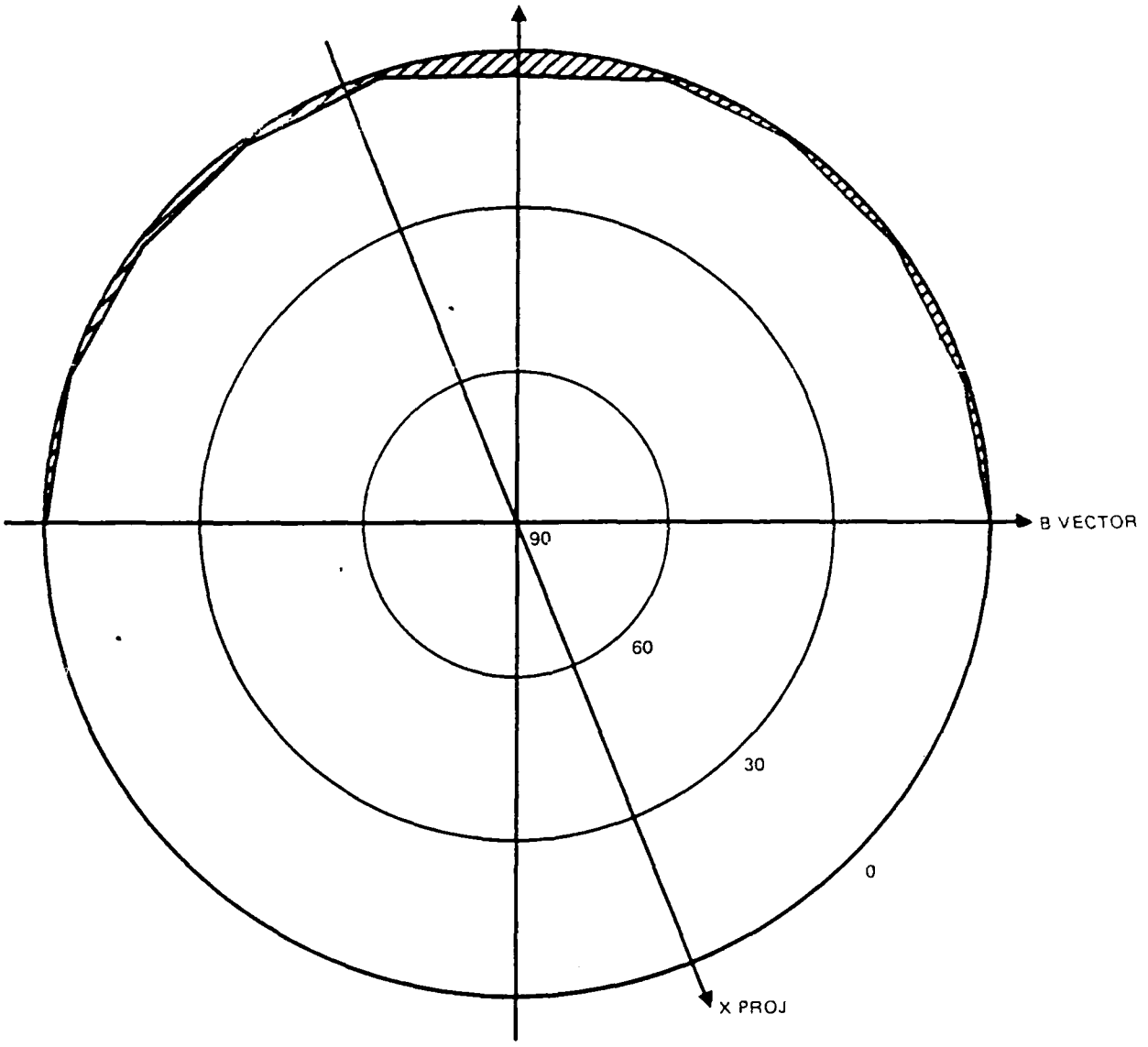

BOUNDARY POSITION: −20.00 −17.90 3.16

ENERGY (KEV) 10 ENTRY FRACTION 0.0084

Figure 3c

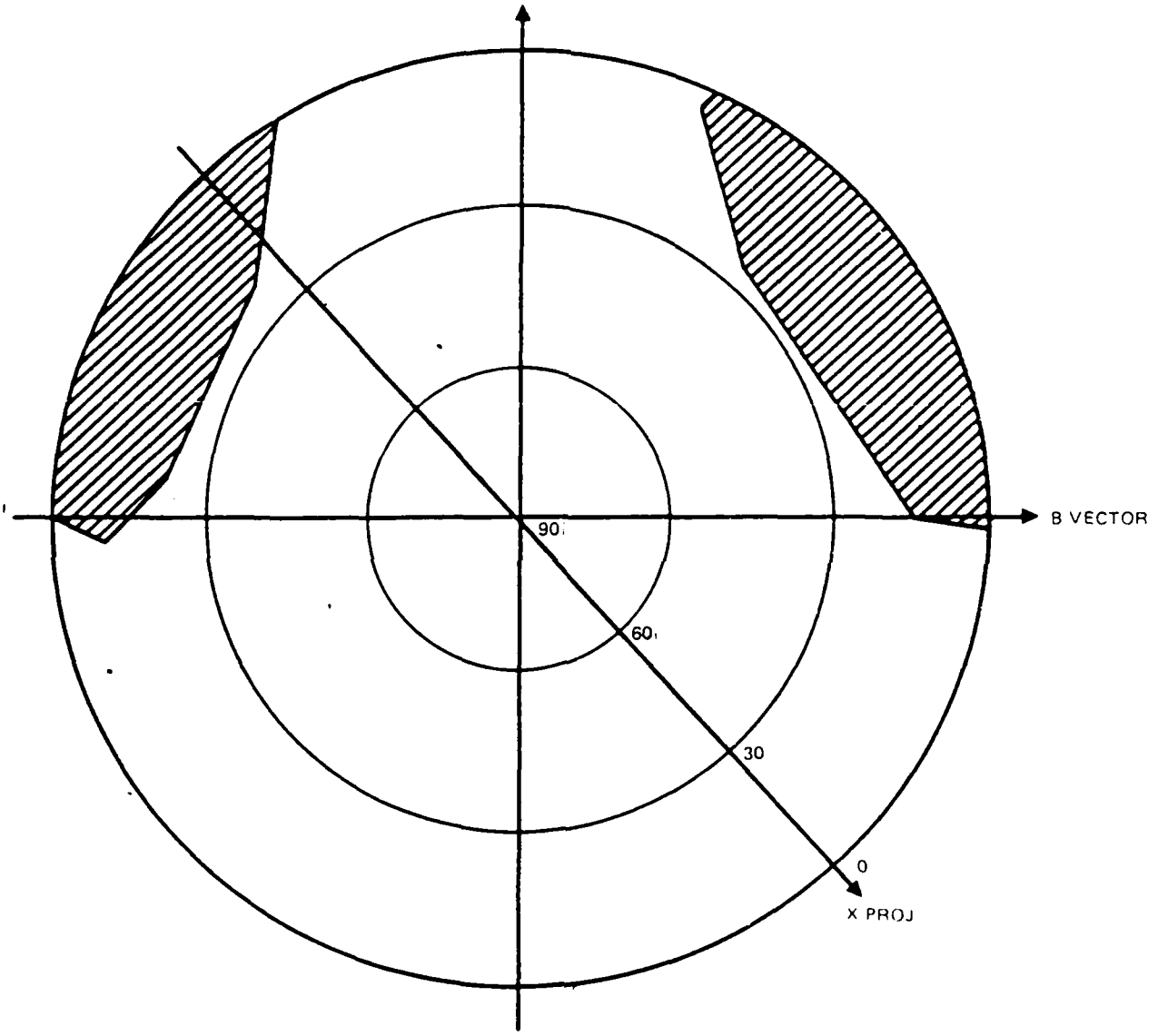

BOUNDARY POSITION: −30.00 −17.44 4.67

ENERGY (KEV): 5 ENTRY FRACTION 0.0572

Figure 3d

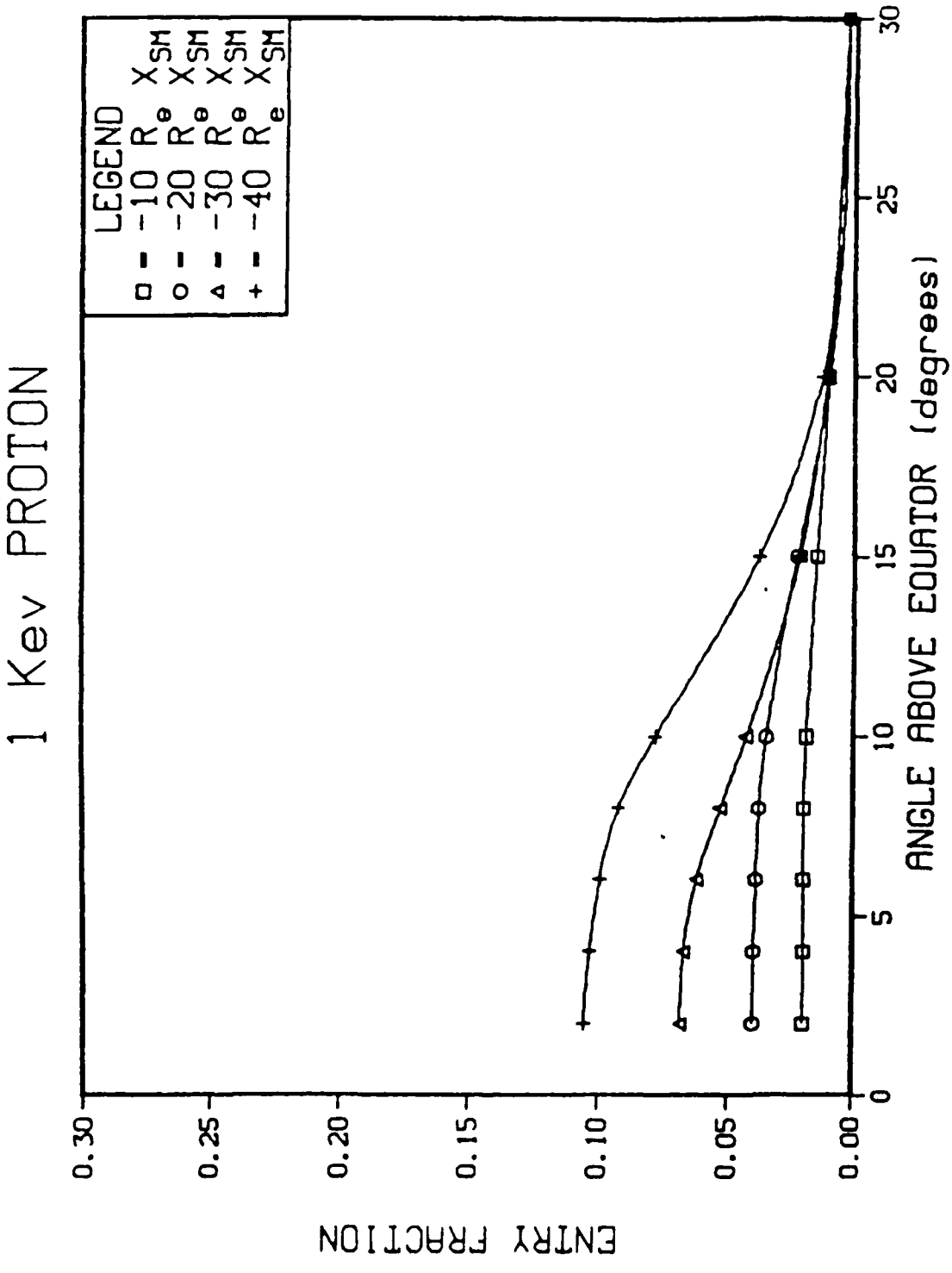
1 Kev PROTON
LEGEND
-10 Re XSM
-20 Re XSM
-30 Re XSM
-40 Re XSM
ENTRY FRACTION
0.30
0.25
0.20
0.15
0.10
0.05
0.00
0
5
10
15
20
25
30
ANGLE ABOVE EQUATOR (degrees)

Figure 4

Entry is strongly dependent on particle energy and location on the magnetopause. The entry fraction increases with distance down the tail, but decreases with distance off the equator. Entry fractions as a function of angle above the magnetic equatorial plane are shown in Figures 4 and 5 for 1 and 10 keV protons. Entry is seen to be confined to a region within 30° of the equator.

Entry fractions for .1 to 10 keV protons are shown in Figure 6. No quantitative work has been performed to date using actual magnetosheath particle distributions. It may be expected, however, that because the magnetosheath plasma flow remains somewhat directed down the tail of the magnetosphere, the entry fraction for the magnetosheath particles may be somewhat larger than the entry fractions determined for an isotropic plasma.

There is another region on the magnetopause where the magnetospheric magnetic field and its gradients are structured such that magnetosheath plasma can gain entry into the magnetosphere. This is on the dayside magnetopause along those field lines that drape back over the lobes of the tail. Particles entering there are constrained to flow along field lines. After entering they therefore either move down the tail or preciptate along field lines into the ionosphere. The flow of entering particles along field lines into the ionosphere constitutes a source of the observed precipitation in the dayside cusp regions. The regions on the magnetopause where appreciable plasma entry occurs are shown schematically in Figure 7.

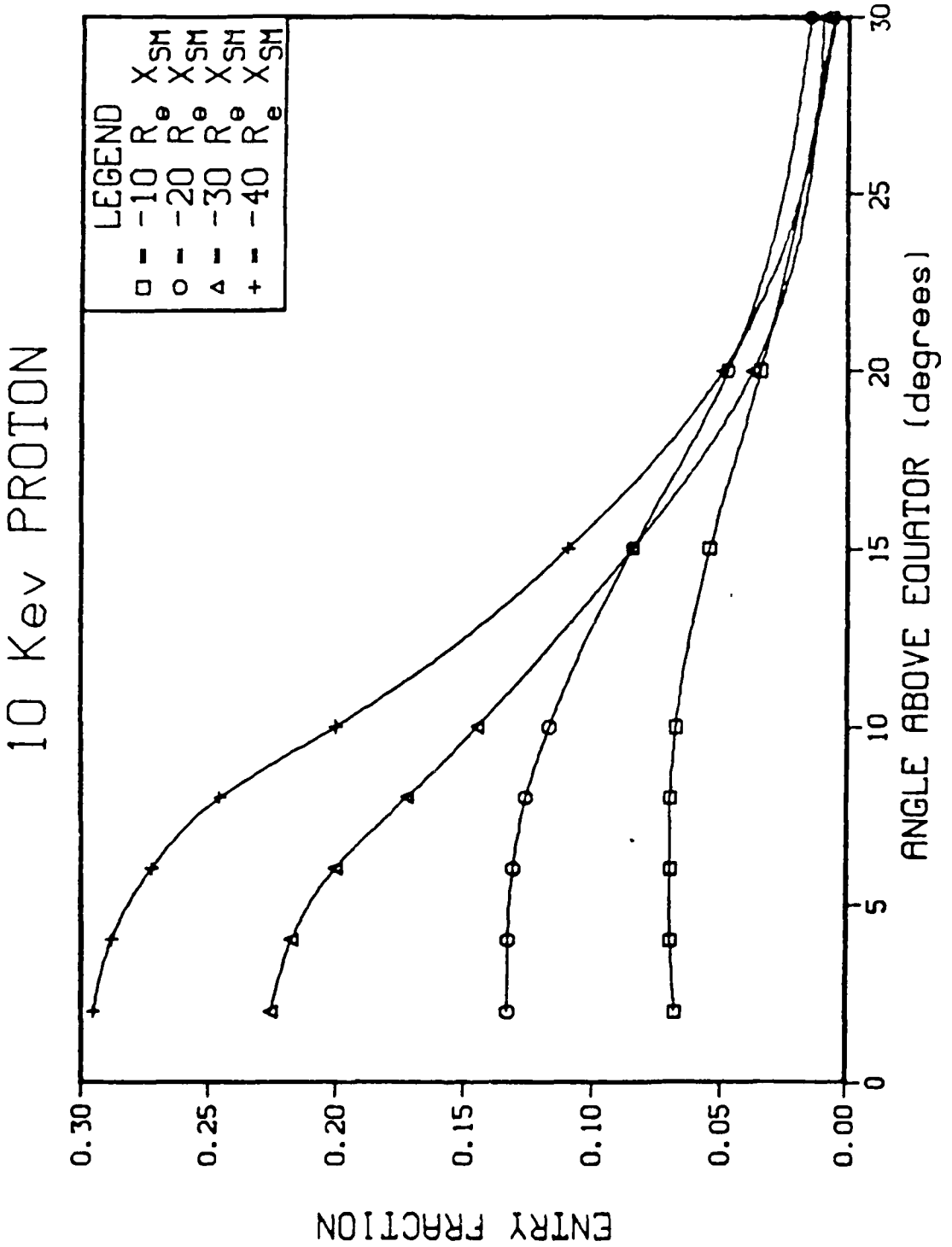
10 Kev PROTON
LEGEND
-10 Re XSM
-20 Re XSM
-30 Re XSM
-40 Re XSM
ENTRY FRACTION
0.30
0.25
0.20
0.15
0.10
0.05
0.00
0
5
10
15
20
25
30
ANGLE ABOVE EQUATOR (degrees)

Figure 5

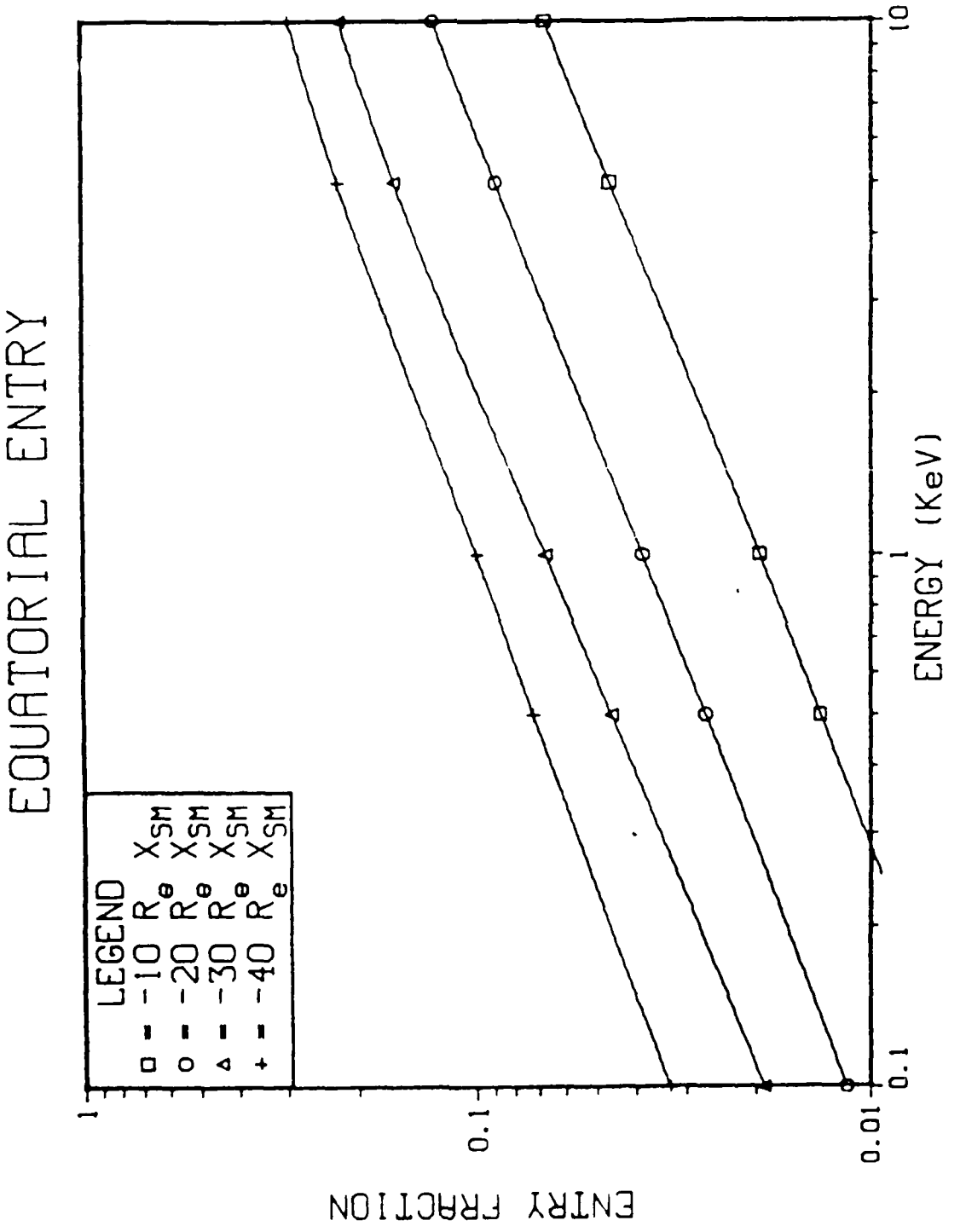
EQUATORIAL ENTRY
LEGEND
-10 Re XSM
-20 Re XSM
-30 Re XSM
-40 Re XSM
ENTRY FRACTION
1
0.1
0.01
0.1
1
10
ENERGY (KeV)

Figure 6

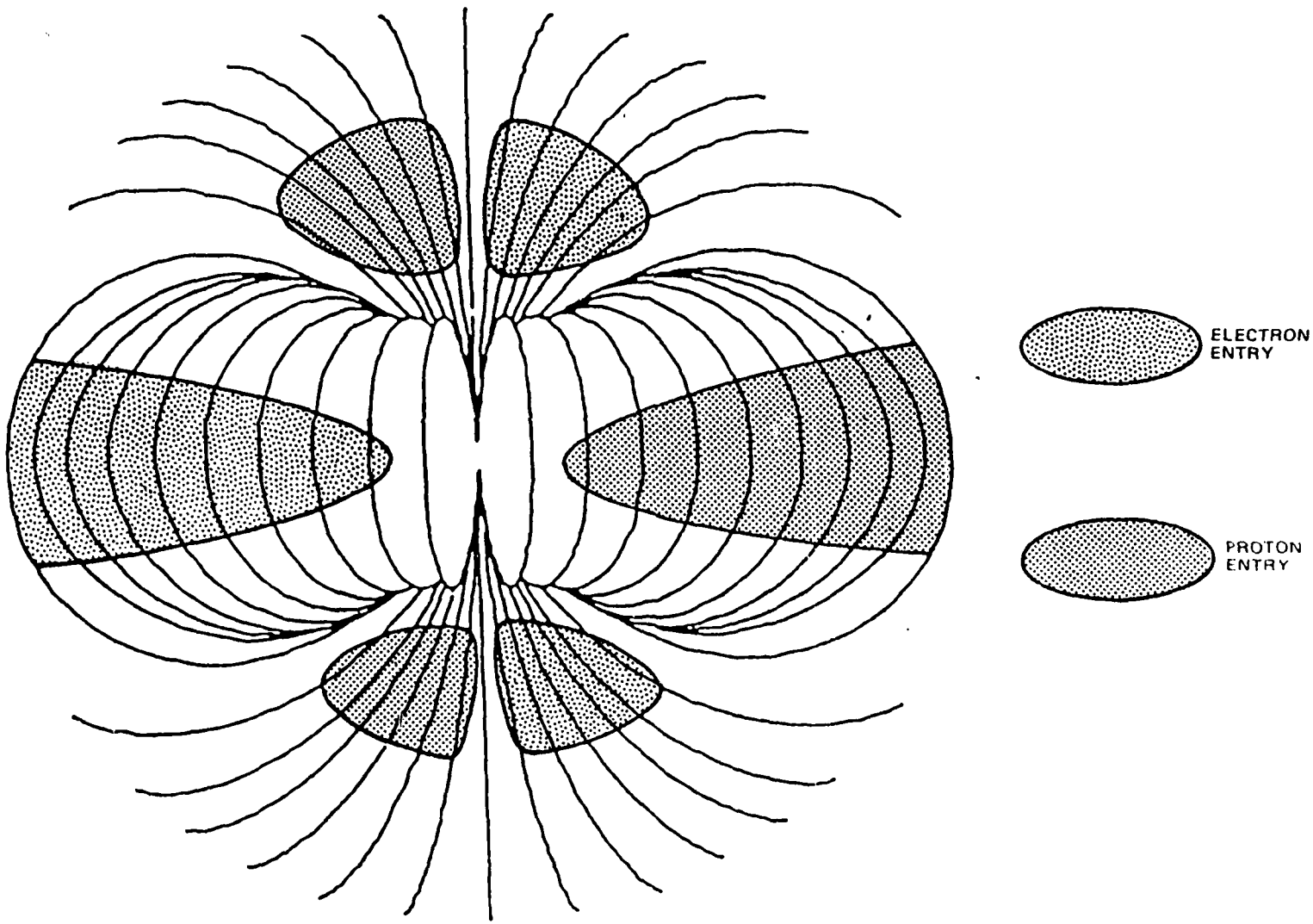

Figure 7

As illustrated in Figure 2, the magnetic field structure limits particle entry such that only protons enter on the dawn side of the magnetosphere and only electrons enter on the dusk side. Since positive ions move clockwise (as viewed from above the equator) in the equatorial region of the tail, their paths move toward the earth on the dawn flank (into a stronger field and therefore decreased gyroradius) and away from the earth on the dusk flank. The opposite is true for electrons. The noon-midnight meridian plane, where the gradient is parallel to $\vec{B}$ by symmetry, (and where, therefore, no entry occurs) separates the two regions. The opposite is true along the field lines poleward of the dayside cusp. There the parallel gradient is the same as in the equatorial region of the tail (the field increasing monotonically with X_{sm}), but the magnetic field direction is reversed. Thus electrons enter on the morning side and positive ions enter in the afternoon side.

Since a fraction of the magnetosheath plasma enters the magnetosphere, the pressure balance between plasma and field at the magnetopause is altered. Thus the pressure balance formalism which assumes specular reflection provides a reasonable value for the scale of the magnetosphere. It follows that the strength and form of the magnetopause currents are also adequately represented by this formalism, as is the gross topology of their associated magnetic field. However, some changes are expected when particle entry occurs. Because of the reduction in magnetosheath pressure resulting from particles entry, it is expected that the tail is slightly wider in the equatorial region than predicted by the old pressure balance theories since particle entry is especially large there.

It is also expected that the real magnetosphere will not contain two neutral points where the total magnetic field is zero, but a more extended region through which the magnetosheath plasma has direct access to the outer magnetosphere. Such a topology is observed.

Although the shape and size of the magnetosphere are not impacted significantly by particle entry, the microstructure of the magnetopause is appreciably changed. Several concepts have been proposed to explain particle entry and energy transfer to this region. They include viscous interaction of the solar wind and magnetospheric magnetic field, the reconnection of the geomagnetic field with the interplanetary magnetic field carried by the solar wind, combinations of the two mechanisms, impulsive events, and anomalous diffusion.

We believe instead that this region is produced simply by the direct entry of charged particles into the magnetosphere and also that the boundary layer is not really separate from the magnetopause. Rather, both the magnetopause and boundary layer are formed by the magnetosheath plasma interaction with the magnetospheric magnetic field, with most of the incident particles being reflected, but a fraction gaining access to the magnetosphere. This magnetopause layer is shown schematically in Figure 8. It is to be contrasted with the magnetopause structure which results from specular reflection. The magnetopause layer can be divided roughly into three regions. In Region 1, all magnetosheath particles are reflected. The magnetopause current flows almost entirely in this region where the incident particles make only a fraction of one circular gyration while in the magnetospheric magnetic field. Region 2 is populated with particles that have not been reflected by the

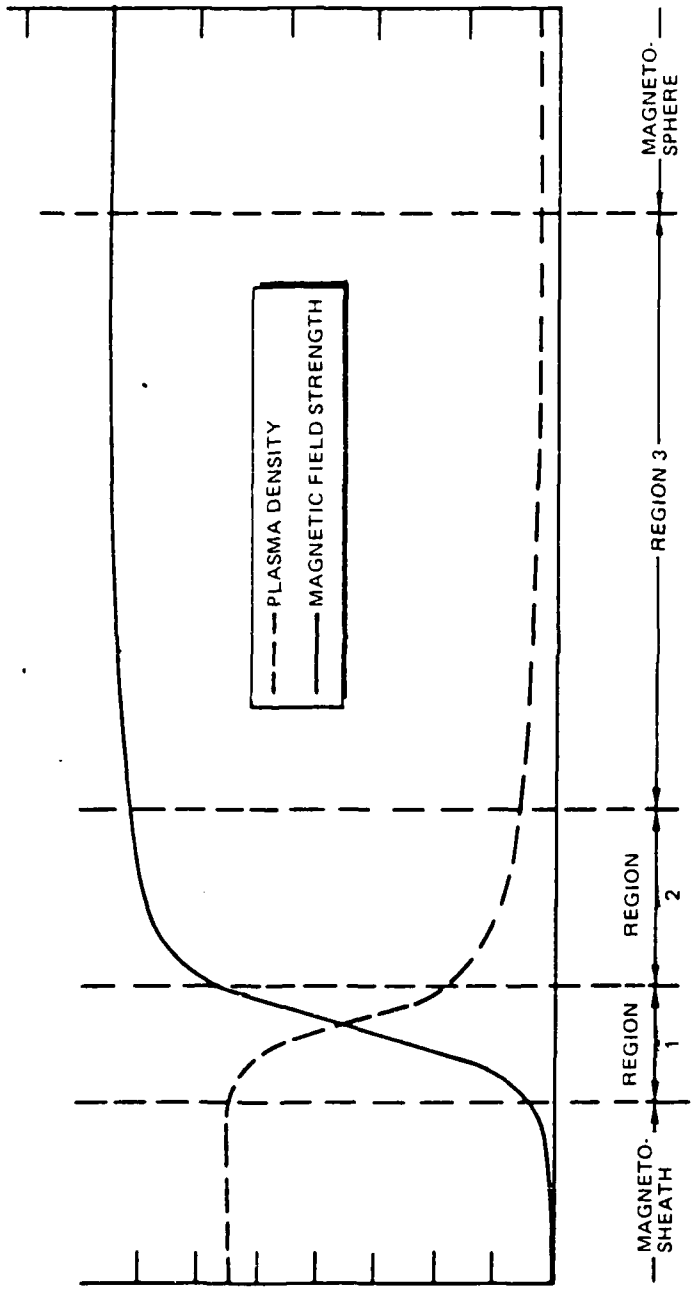
PLASMA DENSITY
MAGNETIC FIELD STRENGTH
MAGNETO-SHEATH
REGION 1
REGION 2
REGION 3
MAGNETO-SPHERE

Figure 8

magnetic field in Region 1. On the dawn side of the tail Region 2 is populated with protons and helium nuclei that have just entered the magnetosphere, and by electrons that have drifted there from the dusk flank and possibly also by electrons from the ionosphere that have moved along magnetic field lines in response to the excess of positive charge in that region. In addition to driving currents, the excess of positive charge in Regions 2 and 3 (on the dawn side) attracts electrons to the region just outside of the magnetopause. This charge separation produces an electric field directed from dusk to dawn across the magnetopause layer. It also produces a dusk to dawn field across the magnetopause layer on the dusk flank. The electric field in the magnetopause layer is shown schematically in equatorial cross section in Figure 9. At the magnetic equator, since $\bar{B}$ is northward, this electric field will produce an antisolar flow of plasma in the magnetopause layer along both dawn and dusk flanks as is observed.

In addition to its influence on the gross shape of the magnetosphere and on the microphysics of the magnetopause, plasma entry continuously influences several large scale magnetospheric features.

As shown in Figures 4 through 6, particle entry in the tail of the magnetosphere is limited to a region near the equator. The motions of particles entering on the flanks of the tail (i.e., near the equator), are responsible for much of the structure of the geomagnetic tail and many of the processes operating there. Once a charged particle has entered the magnetosphere, its subsequent motion is determined in large part by its pitch angle. Particles with pitch angles near zero or 180 degrees (whose motions are parallel or anti-parallel to the magnetic field direction) will move along

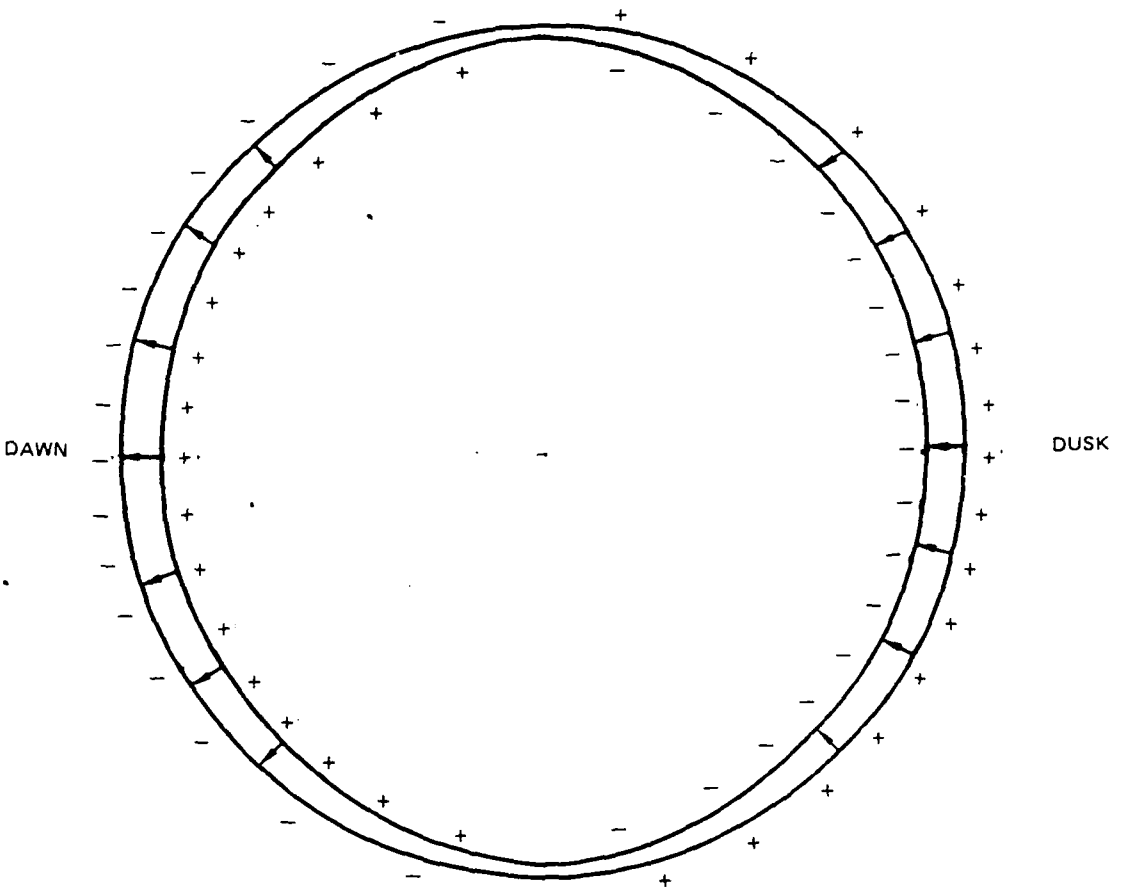

Figure 9

the field line toward the ionosphere. Other particles with pitch angles near 90 degrees (their velocity vector having a large component perpendicular to the magnetic field direction) will be acted upon by the magnetospheric magnetic field and drift across the tail. We believe that the latter group of particles populates the plasma sheet in the tail region. The particles entering the plasma sheet region on the flanks of the tail then drift across the tail, their motions determined by the magnetospheric magnetic and electric fields present there. Magnetic field topology dictates that the plasma sheet is thinner at the center of the tail than at its flank. Also, since equatorial particles follow contours of constant $|\vec{B}|$ the equatorial plasma sheet is formed over the region where these contours intersect the magnetopause (see Figure 10) and thus extends almost to the subsolar magnetosphere.

At the equator on the dawn side, Region 3 of the magnetopause layer should contain primarily protons with pitch angles clustered near 90°. Thus positive charge enters on the dawn side of the tail of the magnetosphere at and near the equator and drifts across the tail. Likewise, electrons enter on the dusk side and drift toward the dawn side, thus forming a cross tail current system. The cross tail currents can also be discussed in terms of gradients in plasma pressure throughout the plasma sheet region. As shown in Figures 4 through 6, the entry of magnetosheath plasma is largest at the magnetic equator in the tail, and falls off dramatically just a few earth radii above or below the equator. Thus it is expected that the plasma density through the plasma sheet is greatest at the equator, and falls off above or below. The plasma pressure gradient profile, taken together with the change in magnetic

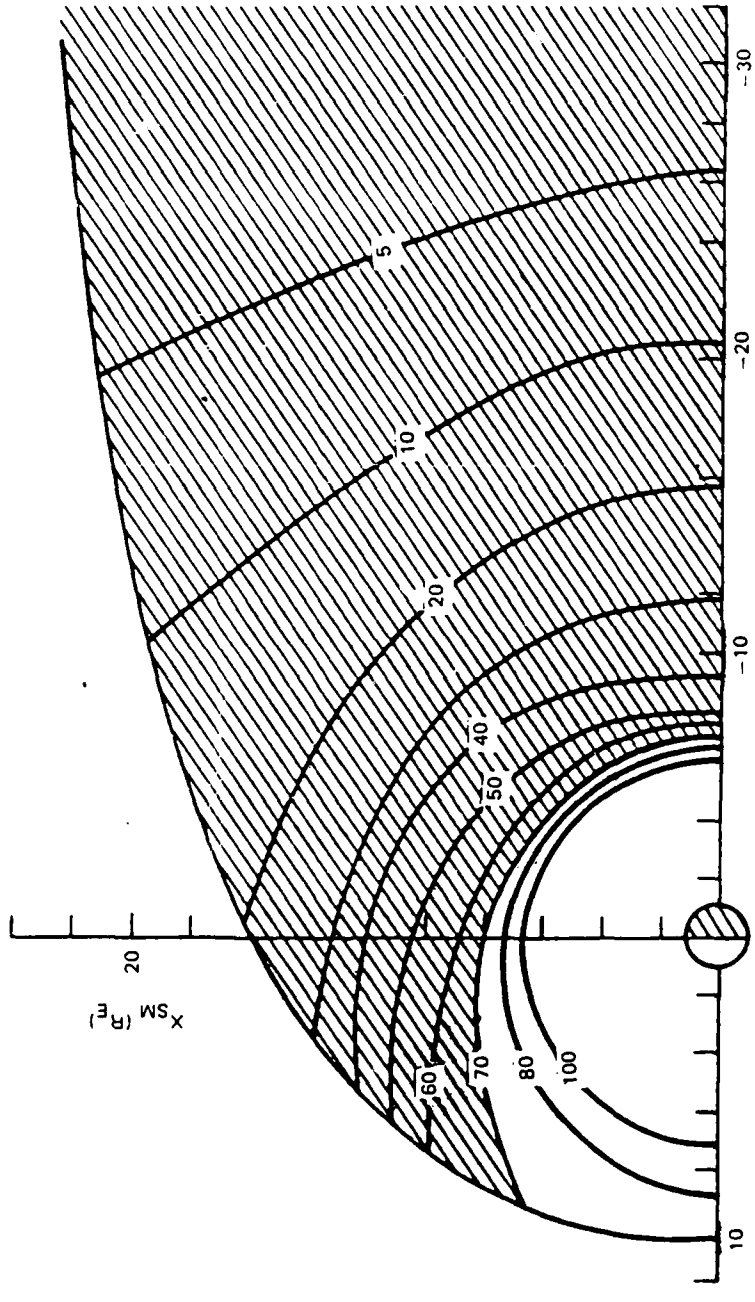

Figure 10

field direction above and below the equator, again suggests that current flows through the plasma sheet on both sides of the magnetic equatorial plane in the dawn to dusk direction.

As discussed above, since only protons enter on the dawn side of the tail of the magnetosphere, an excess of negative charge persists just outside of the dawn magnetopause. The same mechanism produces an excess of positive charge just outside of the dusk magnetopause. We believe that this excess charge on the equatorial flanks of the magnetosphere is dissipated by return currents that are directed from dusk to dawn over the lobe regions just outside of the magnetopause. The plasma sheet, cross tail and return currents, and regions of charge buildup as they occur in the steady state because of direct magnetosheath plasma entry, are shown schematically in planar cross section in Figure 11. For many years this "theta" geometry has been assumed for currents that flow in the tail region since such a current topology is required to explain the observed lobe structure of the tail magnetic field.

Near the equator in the tail particles in the magnetopause layer either drift across the tail or move along field lines to the ionosphere. The drift of protons and electrons across the tail assures that the plasma sheet region is essentially charge neutral. Away from the equator, however, this is no longer true because of the magnetic field topology. Field lines threading the magnetopause layer well above the equator connect to the ionosphere and cross the equator well beyond lunar orbit. Magnetosheath particles which gain access to this region cannot drift into the lobes because they cannot "bounce" along field lines. Thus above and below the equator there is a net accumulation of positive charge on the dawn side and of negative charge on the

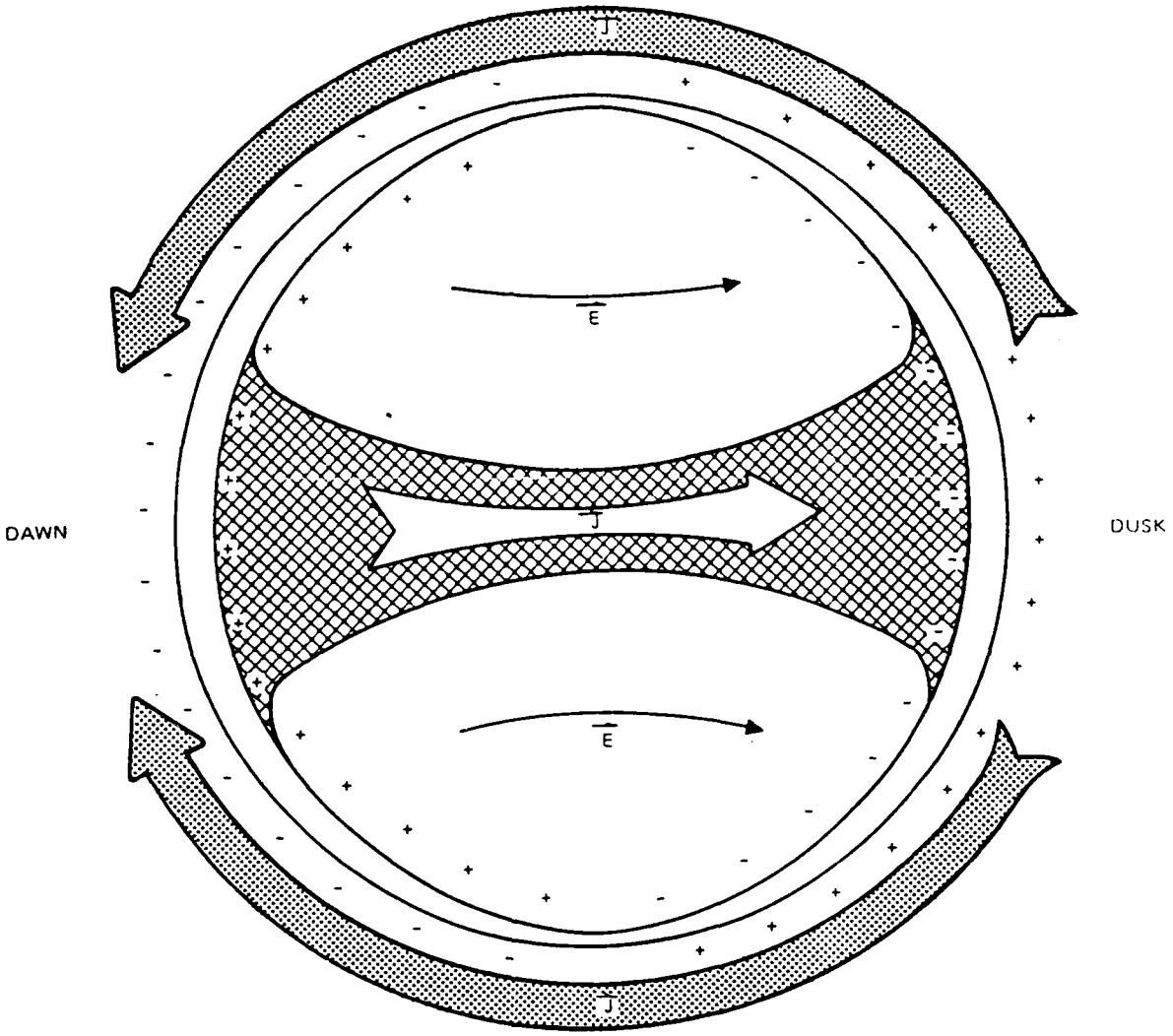

Figure 11

dusk side of the tail. This charge buildup may be dissipated by the flow of current between the magnetopause layer and the ionosphere. However, since charge is continuously being supplied to the sides of the tail of the magnetosphere, it is expected that in the steady state a charge imbalance will persist across the tail. This results in a dawn to dusk electric field across the lobes of the magnetosphere which is also shown schematically in Figure 11. The cross tail electric field may be weaker in the region of the plasma sheet since charge separation between the dawn and dusk flanks of the magnetosphere is not maintained near the equator. Note that this electrostatic field persists from dawn to dusk across the tail at all times. Thus the entry of low energy charged particles into the magnetosphere produces an electric field across the tail of the magnetosphere as required by Axford and Hines to convect the magnetospheric plasma earthward.

The cross section of the tail shown schematically in Figure 11 illustrates all of the features discussed above; the formation of the plasma sheet, the cross tail currents, the cross tail electric field, and the return of the cross tail currents around the lobes of the magnetosphere in the magnetosheath region. None of these features is explained with a pressure balance model that assumes specular reflection. <u>They are all the direct result of the continuous particle entry into the magnetosphere through the magnetopause</u>.

As discussed earlier, once a charged particle has entered the magnetosphere (in Region 2 of the magnetopause layer) its subsequent motion is determined by its pitch angle. Thus on the dawn side of the magnetosphere positively charged particles with pitch angles near 0° or 180° will flow along magnetic field lines toward the auroral ionosphere. Alternatively, charge accumulation

in the dawn magnetopause layer may be shorted out by the flow of electrons from the ionosphere along magnetic field lines. On the dusk side of the magnetosphere the opposite is true. Electrons enter and precipitate along magnetic field lines toward the ionosphere.

The observed location of the Birkeland currents at their junction with the ionosphere is shown in Figure 12. The Region 1 Birkeland currents form two halves of a ring, and are bound by the Region 2 current system that flows at lower latitudes. Note also that near the noon meridian there is a small region of reverse current flow attributed to the precipitation of particles in the dayside cusp regions. It is necessary to use a model of the magnetospheric magnetic field in order to connect these regions in the ionosphere along magnetic field lines to their source regions in the magnetosphere. The locations of field line crossings in the magnetic equatorial plane for lines originating at various magnetic longitudes and latitudes at the earth are shown in Figure 13. This mapping suggests that at least from noon back to the dawn-dusk meridian, the Region 1 Birkeland currents map close to the dawn and dusk equatorial region of the magnetosphere. Thus particle entry occurring at the magnetopause is connected via magnetic field lines to that part of the dayside ionosphere where the Region 1 Birkeland currents are observed to flow. It is more difficult to explain the nighttime Region 1 Birkeland currents. We suggest here only that charged particle entry may again be their source of particles and energy and that the convection of the particles by the cross tail electric field may be an important factor in explaining the nighttime Region 1 Birkeland currents.

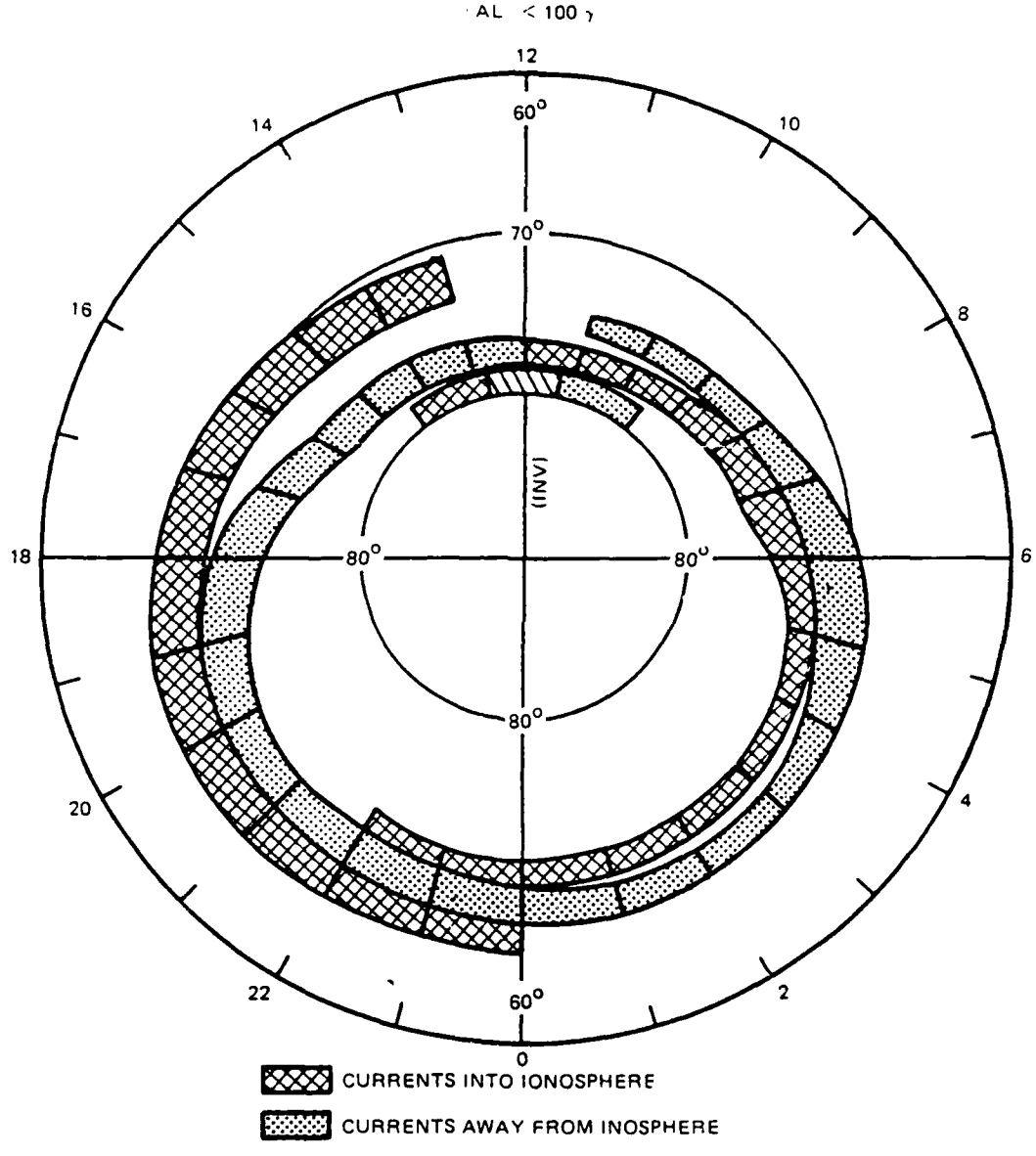

Figure 12

(Redrawn from Iijima, T. and Potemra, T. A., J. Geophys. Res., 81, 5971, 1976.)

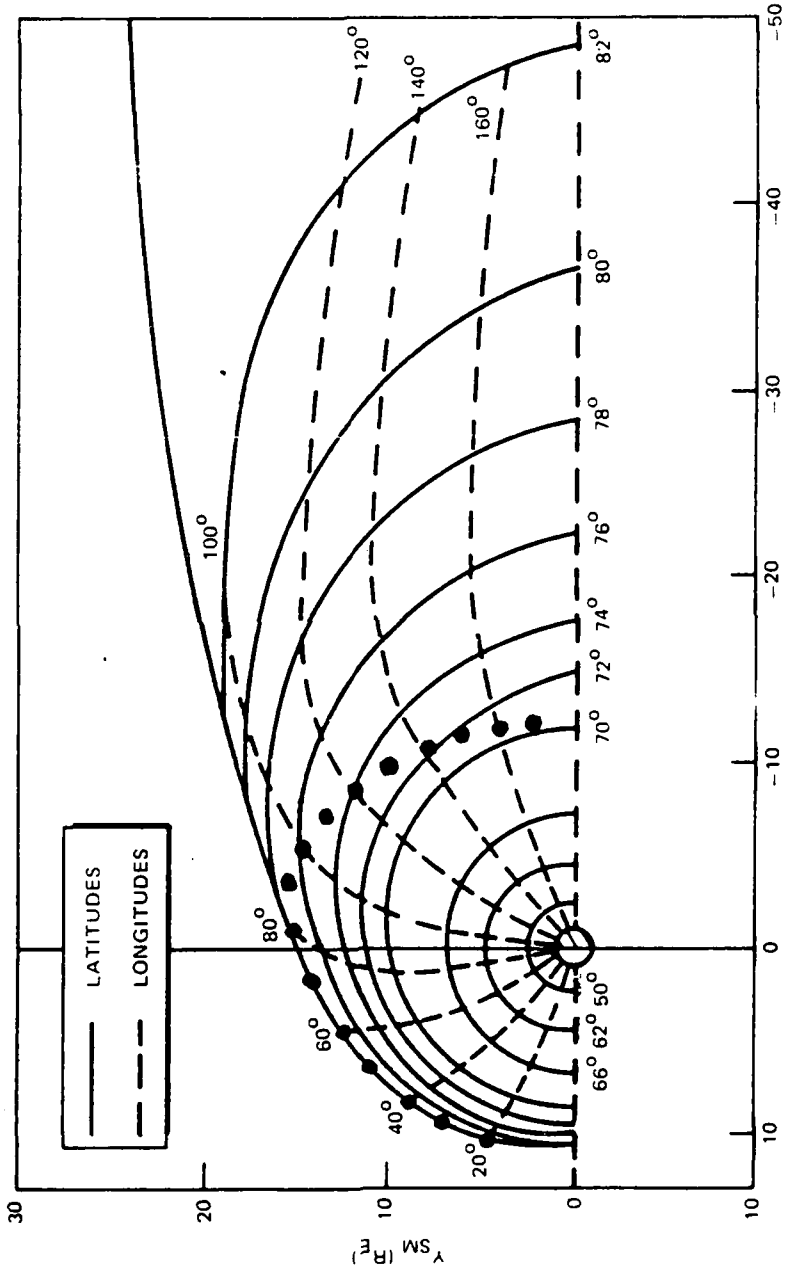
LATITUDES
LONGITUDES
120°
140°
160°
82°
100°
80°
78°
76°
74°
72°
70°
80°
60°
40°
20°
66°
62°
50°
30
20
10
0
10
-50
-40
-30
-20
-10
0
10
Y_{SM} (R_E)
X_{SM} (R_E)

Figure 13

Charged particle entry through the magnetopause also produces currents that flow along the polar side of the dayside cusp region down to the ionosphere. As discussed earlier, although the parallel gradients are directed toward the noon meridian, both on the polar side of the dayside cusp and along the flanks of the tail, the direction of the magnetic field is reversed. Along the flanks of the tail it is everywhere northward, while on the polar side of the dayside cusp the predominant direction of the magnetic field is southward. Thus the species of entering particle is changed and electrons enter on the dawn side, while on the dusk side only positive ions can penetrate the magnetopause. Thus the sense of the currents is reversed from the Region 1 Birkeland currents with electrons flowing toward the ionosphere on the morning side of the magnetosphere, and protons moving toward the ionosphere (or electrons moving out of the ionosphere) on the afternoon side of the magnetosphere. Note that the direction of each of these currents is in agreement with observations of the Birkeland currents (see Figure 12).

The excess of positive charge produced by entry on the dawn side of the magnetopause will either be transmitted along magnetic field lines into the ionosphere, or equivalently, draw electrons out of the ionosphere leaving a deficiency of electrons in the ionosphere where the Birkeland Region 1 field lines intersect the ionosphere. The reverse is true on the dusk side. This charge difference on the two sides of the Region 1 Birkeland currents is in the proper direction to produce a dawn to dusk electric field over the polar cap region, as shown schematically in Figure 14. An electric field in that direction is required to explain the anti-sunward convection of plasma that occurs there more or less continuously.

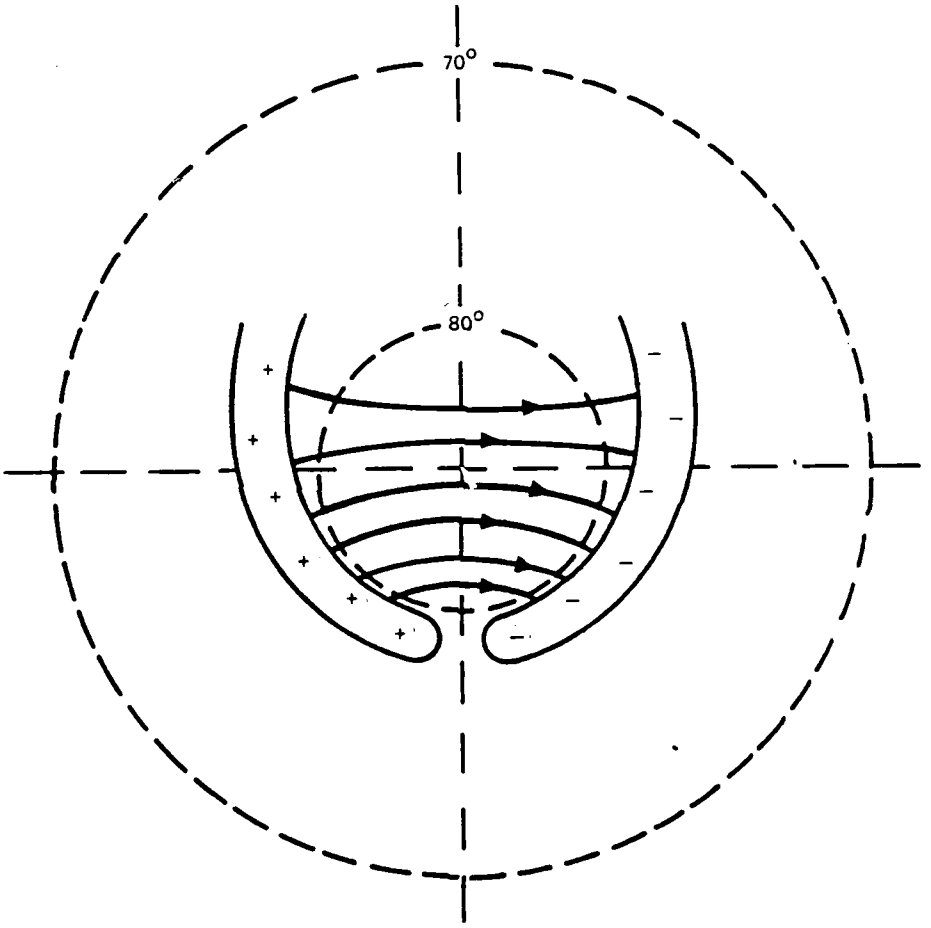

Figure 14

The particle entry process described here in some sense explains the "viscous interaction" suggested by Axford and Hines as the means by which the magnetosphere and solar wind interacted. It produces the cross tail and polar cap electric fields required by Axford and Hines to convect magnetospheric plasma. The entry process also directly drives current systems in the magnetosphere and provides plasma to the tail. The existence of this entry mechanism reduces the demands on the convection process since it directly links the magnetopause layer to the ionosphere (through the Region 1 dayside Birkeland currents) and produces a dawn to dusk electric field across the polar cap.

We have examined the entry of the thermalized solar wind plasma (magnetosheath plasma) into the magnetosphere which occurs at all times because of gradients in the magnetospheric magnetic field parallel to the magnetopause. We believe that this entry process provides the energy and particles required for several known magnetospheric features which persist at all times. These include the plasma sheet and cross tail electric currents, the return currents that flow over the lobes of the tail just beyond the magnetopause, the electric fields directed from dawn to dusk across the tail and across the polar cap, and the dayside Region 1 Birkeland currents. These features, together with the basic magnetopause current system, form the "ground state" of the magnetosphere. This ground state description can be used as the point of departure for studying other magnetospheric processes that depend on the dynamics of the solar wind and interplanetary magnetic field and other plasma phenomena (e.g., wave-particle interactions).

This entry process explains physically the viscous interaction process suggested by Axford and Hines (1961), and also directly supplies plasma to the magnetosphere in the steady state. Because of it the magnetosphere must be considered to be "open" to the entry of a portion of the magnetosheath plasma at all times. This one mechanism produces several magnetospheric currents and fields that are properly directed and is estimated to supply a large enough particle flux to maintain the tail, at least a portion of the Birkeland currents and the dawn to dusk electric field across the tail and the polar cap.

Section 3

TIME VARYING MAGNETIC AND ELECTRIC FIELDS

We have participated actively in two Coordinated Data Analysis Workshops (CDAW's). In CDAW-2, the July 29, 1977 magnetospheric event was scrutinized and we developed a dynamic model for the magnetospheric magnetic and electric fields as they change during that event. More recently, we participated in CDAW-6 where two other magnetospheric events were examined. For CDAW-6, the events were selected such that there was coverage in the tail of the magnetosphere. One of the events covered a very active time, the second event included a relatively isolated substorm. The procedures we followed in developing these models are discussed briefly.

It is emphasized that we did not construct *ad hoc models* to fit a particular event. Rather, we permitted each of the three major magnetospheric current systems to expand and contract in size and strength in response to some physically meaningful input parameter or set of parameters. For example, the size and strength of the magnetopause currents are controlled by the dynamic solar wind pressure. The input parameters used for each of the three current systems and the scaling laws employed in the development of the model are discussed in his section. A key part of the procedure is the determination of a "strength factor", S, which is used to describe the variability of each of the three current systems. Thus the strength factor is the link between the physical input parameters and the magnitude of the current system.

The strength and size of the magnetopause currents are determined using a pressure balance equation which relates the kinetic pressure of the solar wind to the magnetic energy density of the magnetic field inside the magnetopause. Most of the variability in the solar wind pressure is caused by changes in the density of the solar wind. (The solar wind velocity seldom drops below 250 km/sec and has only rarely been observed above 1000 km/sec.) The pressure balance formalism leads directly to a standoff distance for the magnetopause.

$$R_s(t) = [M^2/(4\pi\ \rho V^2)]^{1/6} \qquad (1)$$

Changes in the standoff distance, $R_s(t)$, and thus size of the magnetosphere are caused by changes in solar wind pressure.

Pressure balance formalism also provides a direct relation between the strength of the magnetopause currents and solar wind pressure. The magnetopause currents produce a field outside of the magnetosphere that cancels the fields generated within the magnetosphere, the largest being the earth's main (dipolar) field, which decays as the inverse cube of the distance from the center of the earth. The variation in the strength of the magnetopause currents is inversely proportional to the cube of the standoff distance.

It was possible to use ground-based magnetic indices in the analysis to help represent variations in the ring current. Traditionally, D_{st} measured at mid-latitudes is considered the best index for representing variations in the strength of the ring current. D_{st} is simply the storm time deviation from the nominal quiet time field at mid-latitudes produced by changes in the

magnetospheric currents during a storm. Since an accurate representation of the magnetopause magnetic field was already available, it was possible to develop a simple algorithm for removing the effects of the changing magnetopause currents from D_{st}. In the quiet time model, the field from the magnetopause near the vicinity of the earth is 25 nanotesla (nT). This quiet time value is part of the D_{st} baseline and is thus the zero level for the D_{st} contribution.

The quiet ring current, $\vec{J}_R$ is represented initially by a series of wire loops. The field from the westward portion of the ring flowing outside of L = 2.5 (which is presumably the portion of the ring enhanced during a storm) contributes about -40 nT to the field at the earth.

When the magnetopause is compressed, only the outer edges of the ring are compressed. Since the largest contribution of the ring (i.e., the strongest currents) are near L's of 3 or 4 the size of the ring was not scaled. This leads to an error in evaluating the contribution from the ring. However, until additional data on changes in $\vec{J}_R(t)$ become available, very little improvement over this approach can simply and accurately be made. Based on comparisons of these model results with observations, however, we feel that this approach gives a reasonable representation of the storm time ring current system.

The tail currents were tied directly to the magnetopause currents. We have also used the so-called epsilon index which multiplies the Poynting vector of the interplanetary electromagnetic field (as observed in a magnetospheric reference system) by a geometry factor which attempts to represent the cross section of the magnetosphere to this energy input.

The suggested relationship of tail current strength to the epsilon index is that the strength factor for the tail currents, $S_T(t)$, be given by $S_T(t) = .15\ \varepsilon$ and if $S_T(t) < 1$ then $S_T(t) = 1$, where $S_T(t)$ is the strength of the tail current system relative to quiet times. The "if test" is required because it is believed that the tail currents are present even when ε is zero). Since the tail current system must fit inside the compressed magnetosphere the position scaling relationship used for the magnetopause was also used for the tail current sytems.

Using the inputs described above to specify the changes in strength of the major magnetospheric current systems during the event, it was possible to vectorally add the contributions to the magnetospheric magnetic field and to then test the accuracy of the model by comparisons with observational data. Again, we emphasize that no observational magnetic field data were used in the construction of this event model. In Figure 15, model data are compared with observations at the orbit of the geosynchronous satellite GOES 1 for the July 29 event. It is seen that the H and the D components agree reasonably well, whereas the V component which gives a measure of the tail-like nature of the field observed at the satellite suggests that the field is more tail-like than the model predicts. Note that some of the substorm structure observed is, indeed, included in the model event. Also, it is not expected that the fit would be perfect, since the model input data were based on hourly or one-half hour averages and does not include parallel currents.

At CDAW-6, the situation was somewhat different. We found that our models very adequately represented the total magnetospheric magnetic field on the dayside of the magnetosphere; however, near midnight the agreement breaks down

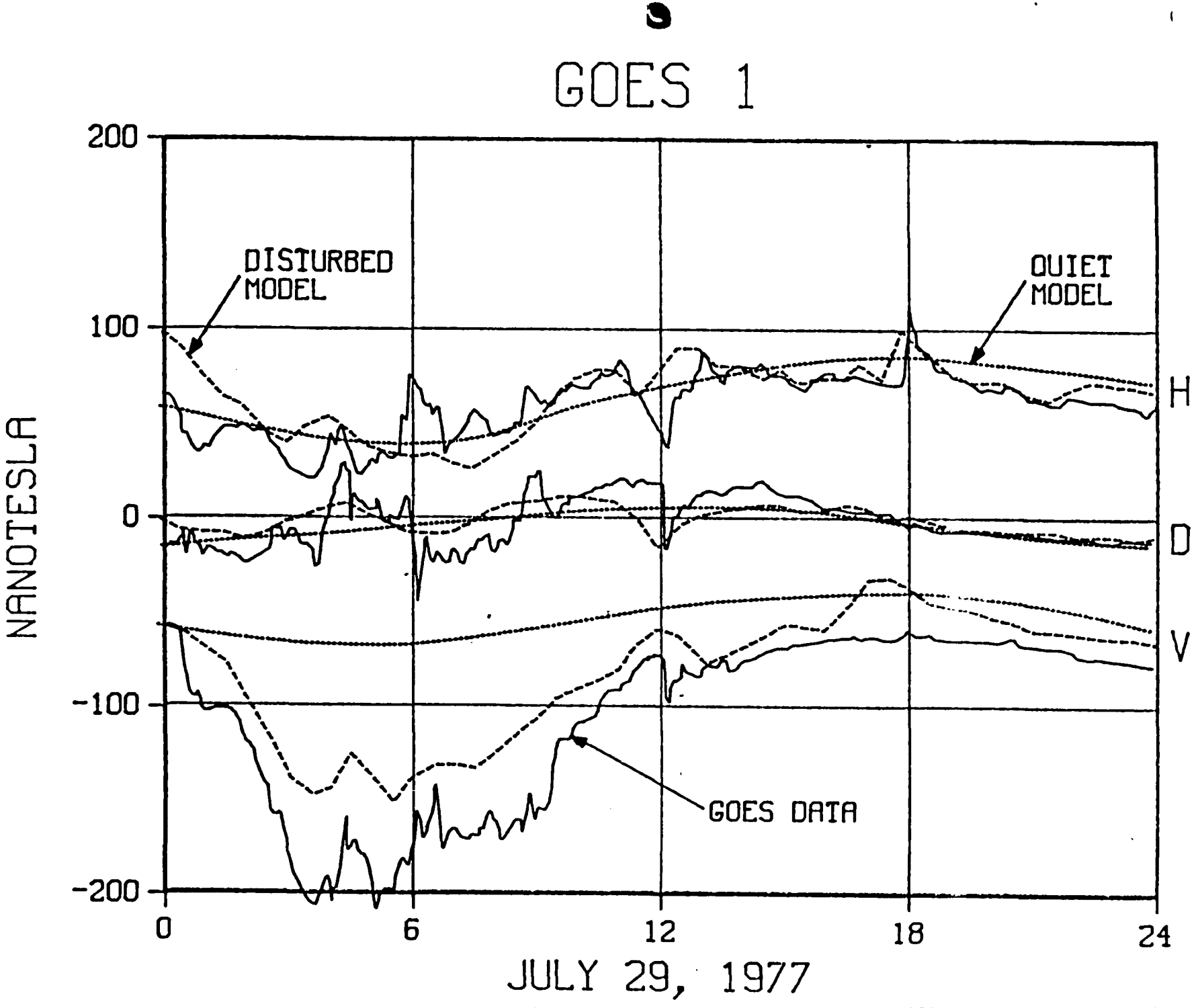
GOES 1
200
100
0
-100
-200
NANOTESLA
DISTURBED MODEL
QUIET MODEL
H
D
V
GOES DATA
0
6
12
18
24
JULY 29, 1977

dramatically. We tried to change the strength of the tail current system, and even its location in order to explain this discrepancy, but were not successful. We now believe that the closure of the Birkeland Region 2 currents near the inner edge of the plasma sheet is a major contributor to the magnetic field in the region of synchronous orbit near midnight, especially during disturbed magnetospheric conditions. Note that although the tail current circuit of approximately 2 million amperes is distributed over several tens of earth radii. The closure of the Birkeland Region 2 currents is confined to a region on the order of 1 or 2 earth radii. Thus the Birkeland Region 2 currents are much more concentrated in the tail currents, and it is expected that their magnetic signature is quite pronounced near the inner edge of the plasma sheet. A comparison of our event model with data for the March 22, 1979 event is shown in Figure 16.

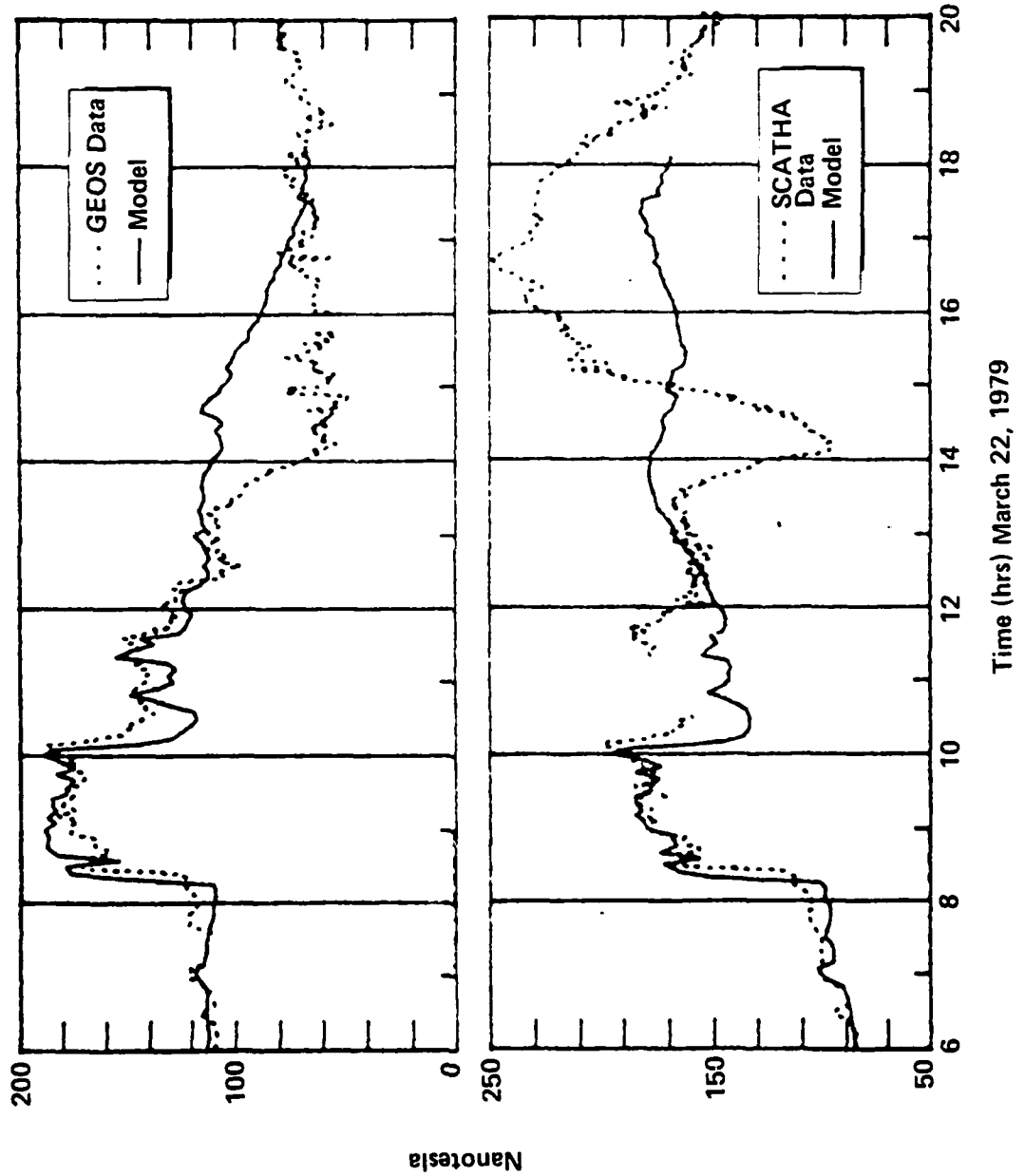
GEOS Data
Model
SCATHA
Data
Model
Nanotesla
200
100
0
250
150
50
6
8
10
12
14
16
18
20
Time (hrs) March 22, 1979

Figure 16

Section 4

PROCEDURE FOR MAPPING ELECTRIC FIELDS FROM IONOSPHERIC TO SATELLITE ALTITUDES

The measurement of dc electric fields is at best difficult. Data from several boom experiments that have been collected over the past decade are now considered by many researchers to be suspect. Thus several investigators have attempted to "map" the electric field from one region of the magnetosphere to the other along magnetic field lines, usually using the assumption that the magnetic field lines are electric equipotentials. We have worked with several other investigators active in the CDAW workshops in an effort to map electric fields from the ionosphere to satellite altitudes. In particulr, the STARE radar data set provides information on the electric field in the ionosphere. The magnetic footprint of the GEOS 2 satellite lies within the STARE radar grid much of the time. It is therefore possible to map the measured electric field in the ionosphere to the GEOS satellite, which is at geosynchronous orbit. The GEOS satellite has two dc electric field experiments. One uses an electron gun, and attempts to determine the electric field by measuring the motion of various energy particles in a combined magnetic and electric field. The other experiment is a boom experiment which examines the difference in potential between two spheres separated by long booms. If a good correlation can be found between the STARE radar electric field data and either of the data sets from the GEOS 2 satellite, it would confirm that the particular electric field experiment was valid, and also that the mapping procedures are accurate.

The assumption that has been generally used in mapping the electric field is that the conductivity along field lines is high and thus the field lines are equipotentials. Hones and Bergeson have stated that the high conductivity assumption implies that the total electric field parallel to the field lines is zero. The electric field equal zero condition is not the same as the equipotential condition since the total electric field, $\bar{E}_T$, at any given point is given by

$$\bar{E}_T = -\frac{1}{c}\frac{\partial \bar{A}}{\partial t} - \nabla\phi \qquad (2)$$

where ϕ is the electric scalar potential, $\bar{A}$ is the magnetic vector potential, and c is the speed of light.

From this equation we see that the electric field consists of an induction electric field and a scalar potential term. In the limit as the induction field goes to zero, the electric field equals zero constraint approaches the equipotential constraint. However, the induction term is never zero. Even during magnetically quiet times the non-aligned dipoled axis causes a $\partial\bar{A}/\partial t$ from the internal field, as well as $\partial\bar{A}/\partial t$ from the magnetospheric currents responding to the wobbling dipole. During magnetically disturbed times the induced field may be quite large. Here, we define a new mapping procedure that does not use a parallel electric field constraint. It is used to evaluate the effects of $\partial\bar{A}/\partial t$ during quiet and disturbed times.

The constraint that there be no parallel electric field can be stated as

$$\bar{E}_T \cdot \hat{B} = 0 \tag{3}$$

where $\bar{E}_T$ is the total electric field and $\bar{B}$ is the unit magnetic field vector. Since we know that

$$\bar{E}_T = - \nabla\phi - \frac{1}{c} \frac{\partial \bar{A}}{\partial t} \tag{4}$$

Then

$$\bar{E} \cdot \hat{B} = - \nabla\phi \cdot \hat{B} - \frac{1}{c} \frac{\partial \bar{A}}{\partial t} \cdot \hat{B} = 0 \tag{5}$$

Therefore

$$\nabla\phi \cdot \hat{B} = - \frac{1}{c} \frac{\partial \bar{A}}{\partial t} \cdot \hat{B} \tag{6}$$

$$\nabla\phi \cdot \hat{B} \equiv \frac{d\phi}{ds} = - \frac{1}{c} \frac{\partial \bar{A}}{\partial t} \cdot \hat{B} \tag{7}$$

where $d\phi/ds$ is the change of ϕ along a field line direction. Thus $\nabla\phi$, the change in ϕ, between two points A and B along a field line is given by

$$\nabla\phi = \int_A^B -\frac{1}{c}\,\frac{\partial \bar{A}}{\partial t} \cdot \hat{B}\, ds \qquad (8)$$

Equation (8) provides a procedure for determining the change in ϕ anywhere along a field line in the presence of a $\partial\bar{A}/\partial t$. To evalute the total electric field, $\bar{E}$, at a point, one needs a boundary condition on ϕ perpendicular to the lines of force. Here it is assumed that the potential (or potential electric field) is known over the ionosphere.

Given the electric field over some region of the ionosphere, the electric field at a satellite can be determined providing the foot of the field line from the satellite is within the ionospheric grid over which the ionospheric electric field is known. It is not practical to start the field line integral in the ionosphere and find the satellite point. It is much simpler to begin the integration procedure at the satellite and determine the intersection within the ionospheric grid.

Since the mapping procedure yields only potentials, it is necessary to map three field lines from the satellite to the ground. The potential difference betwen these field lines can then be used to determine the electric field. Figure 17 defines three such field lines. Given that the satellite is located at point A a distance $\bar{R}_A$ from the center of the earth, points C and C' are a distance $\Delta\bar{r}_{AC}$ and $\Delta\bar{r}_{AC'}$ respectively from point A. $\Delta\bar{r}_{AC}$ and $\Delta\bar{r}_{AC'}$ are perpendicular to the magnetic field at point A and $\Delta\bar{r}_{AC}$

$$E_{AC} = \frac{\vec{E}_B \cdot \Delta\vec{r}_{BD}}{|\Delta\vec{r}_{AC}|} + \frac{V_{CD} - V_{AB}}{|\Delta\vec{r}_{AC}|}$$

$$E_{AC'} = \frac{\vec{E}_B \cdot \Delta\vec{r}_{BD'}}{|\Delta\vec{r}_{AC'}|} + \frac{V_{CD'} - V_{AB}}{|\Delta\vec{r}_{AC'}|}$$

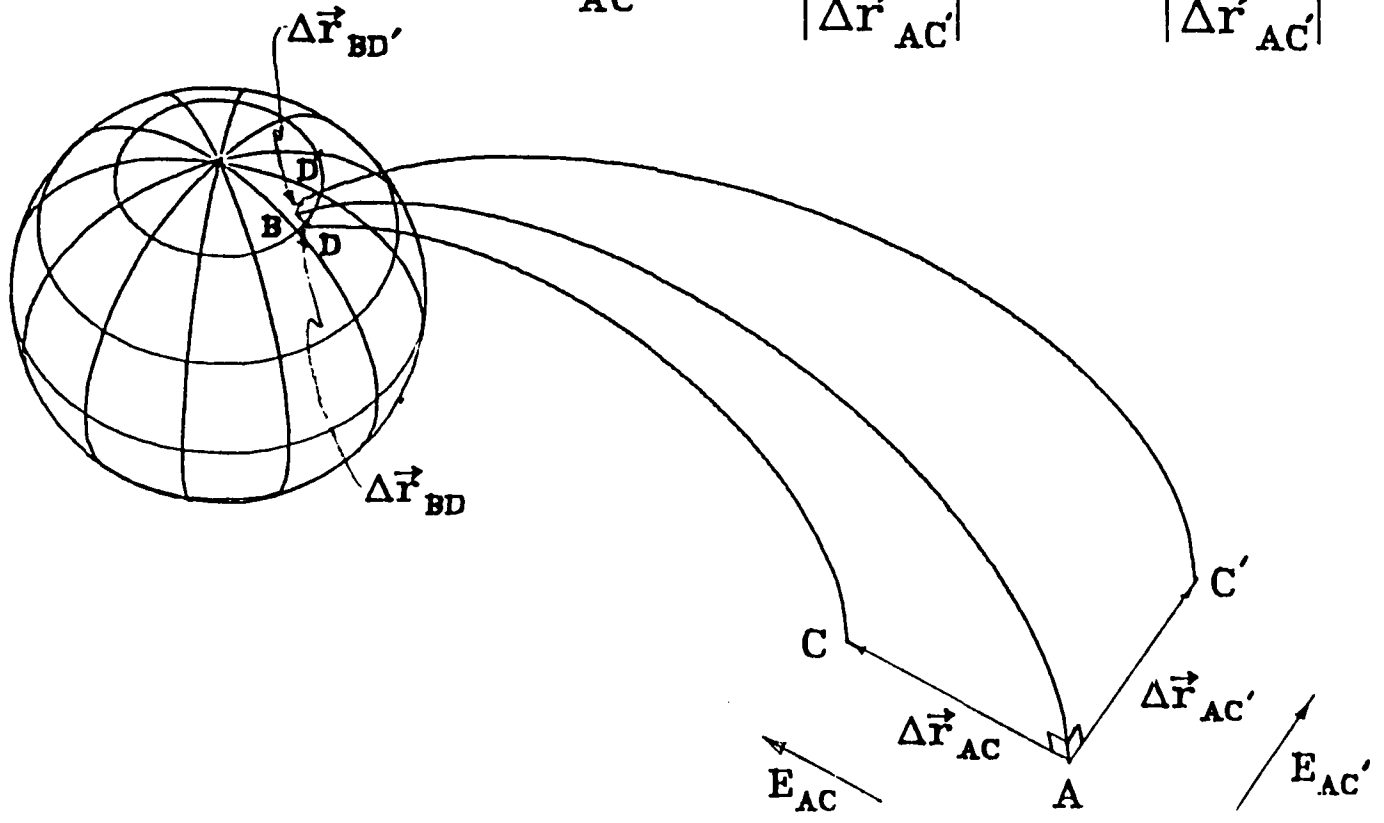

Figure 17

and $\Delta\bar{r}_{AC'}$ are perpendicular to each other. Thus if the potentials at points A, C and C' are evaluated, the potential electric field in the $\Delta\bar{r}_{AC}$ and $\Delta\bar{r}_{AC'}$ direction can be determined ($E = -\Delta V/\Delta r$).

If point B is the conjugate point in the ionosphere (of the field line passing through point A), we can define a plane through point B perpendicular to magnetic field at point B. Points D and D' are then the conjugate points of C and C' respectively in this perpendicular plane and $\Delta\bar{r}_{BD}$ and $\Delta\bar{r}_{BD'}$ are the distance vectors between B and D, and B and D' respectively. Finally, $\bar{R}_B$, $\bar{R}_D$ and $\bar{R}_{D'}$ are the locations of points B, D and D' with respect to the center of the earth.

If we begin the integral of equation (8) at point A and integrate to B, we obtain

$$\Delta\Phi_{AB} = V_{AB} \tag{9}$$

where V_{AB} is the potential of point B with respect to A. Similar integrals starting at points C and C' give

$$\Delta\Phi_{CD} = V_{CD} \tag{10}$$

$$\Delta\Phi_{C'D'} = V_{C'D'} \tag{11}$$

The potential V_{CD} is the potential at point D with respect to C and $V_{C'D'}$ is the potential at point D' with respect to C'.

If the potential electric field in the ionosphere is known to have the value $\bar{E}_I$ in the inertial frame, and V is the potential in the initial frame

$$\bar{E}_I = - \nabla V \quad , \quad \text{and therefore} \tag{12}$$

$$\Delta V_{BD} = - \bar{E}_I(\bar{R}_B) \cdot \Delta\bar{r}_{BD} \tag{13}$$

where ΔV_{BD} is the potential of point D with respect to B, and where $\bar{E}_I(\bar{R}_B)$ is the potential electric field at point B. If we arbitrarily define point B as having a potential V_o, then

$$V_B = V_o \tag{14}$$

$$V_D = V_o - \bar{E}_I(\bar{R}_B) \cdot \Delta\bar{r}_{BD} \tag{15}$$

$$V_A = V_B - V_{AB} \tag{16}$$

$$V_C = V_D - V_{CD} \tag{17}$$

The electric field E_{AC} at point A in the direction $\Delta\bar{r}_{AC}$ is then

$$E_{AC} = - \frac{V_C - V_A}{|\Delta\bar{r}_{AC}|} \tag{18}$$

$$= \frac{V_A - V_C}{|\Delta\bar{r}_{AC}|} \tag{19}$$

$$E_{AC}(\bar{R}_A) = \frac{V_B - V_{AB} - (V_D - V_{CD})}{|\Delta\bar{r}_{AC}|} \tag{20}$$

$$= \frac{V_B - V_D + V_{CD} - V_{AB}}{|\Delta\bar{r}_{AC}|} \tag{21}$$

$$= \frac{V_o - (V_o - \bar{E}_I(\bar{R}_B) \cdot \Delta\bar{r}_{BD}) + V_{CD} - V_{AB}}{|\Delta\bar{r}_{AC'}|} \tag{22}$$

$$= \frac{\bar{E}_I(\bar{R}_B) \cdot \Delta\bar{r}_{BD}}{|\Delta\bar{r}_{AC}|} + \frac{V_{CD} - V_{AB}}{|\Delta\bar{r}_{AC}|} \tag{23}$$

Similarly in the electric field in the $\Delta\bar{r}_{AC'}$ direction is given by

$$E_{AC'}(\bar{R}_A) = \frac{\bar{E}_I(R_B) \cdot \Delta\bar{r}_{BD'}}{|\Delta\bar{r}_{AC'}|} + \frac{V_{C'D'} - V_{AB}}{|\Delta\bar{r}_{AC'}|} \tag{24}$$

The above equations for E_{AC} and $E_{AC'}$ are the basic mapping equations for mapping the ionospheric electric field from the ionosphere to the satellite in the presence of a $\partial\bar{A}/\partial t$ when the $\bar{E}\cdot\hat{B} = 0$ condition (conducting field lines) is satisfied. When $\partial\bar{A}/\partial t$ is zero, the second terms in equations (23) and (24) vanish and one has the standard equipotential mapping terms.

The equipotential mapping states that the electric field at the satellite is the corresponding electric field in the ionosphere multiplied by the ratio of distance between the field lines in the magnetosphere. We note when $\partial\bar{A}/\partial t \neq 0$ that the result will differ from the equipotential approach.

Inertial/Rotating Reference Frames

The results of the previous section are rigorously true only in an inertial reference frame. Thus $\bar{E}_I$ must be specified in an inertial frame and E_{AC} and $E_{AC'}$ are the results in the inertial reference frame. $\bar{E}_I$, the ionospheric electric field, is the scalar potential electric field in the inertial reference frame.

A computer program was written that allowed us to perform the integral in equation (8) and evaluate V_{AB}. V_{CD}, and $V_{CD'}$ in an arbitrary magnetic field and an arbitrary $\partial\bar{A}/\partial t$. We have examined several cases.

Hones/Bergeson Case. Hones and Bergeson solve the case of a rotating conducting magnetized sphere in which the dipole axis is not aligned with the rotation axis. We define an inertial coordinate system in which the sphere rotates with an angular velocity, $\bar{\omega}$. For simplicity, the rotation axis is

aligned with the z axis of the coordinate system. The magnetic dipole $\bar{\mu}$ makes a finite angle with the rotation vector ω.

It can be shown that

$$\bar{A} = \frac{\bar{\mu} \times \bar{r}}{|\bar{r}|^3} \tag{25}$$

$$\bar{B} = \frac{3\,\bar{r}\,(\bar{r}\cdot\bar{\mu}) - \bar{\mu}\,(\bar{r}\cdot\bar{r})}{|\bar{r}|^5} \tag{26}$$

$$\frac{1}{c}\,\frac{\partial \bar{A}}{\partial t} = \frac{-1}{c|r|^3}\,[\bar{r} \times (\bar{\omega} \times \bar{\mu})] \tag{27}$$

Hones Bergeson showed that the self-consistent potential on the sphere as seen from the inertial frame that satisfies the $\bar{E}\cdot\hat{B} = 0$ condition is

$$V = \frac{1}{ca^3}\,(\bar{\omega} \times \bar{r})\cdot(\bar{\mu} \times \bar{r}) \tag{28}$$

where a is the radius of the sphere. One can evaluate the electric field on the sphere, $\bar{E}_I = -\nabla V$, and get

$$\bar{E}_I = -\nabla V = -\nabla\,[\frac{1}{cr^3}\,(\bar{\omega} \times \bar{r})\cdot(\bar{\mu} \times \bar{r})] \tag{29}$$

Evaluating this gradient and substituting in value from equations (26) and (27) gives

$$\bar{E}_I(\bar{R}_B) = + \frac{1}{c} \frac{\partial \bar{A}}{\partial t} - \frac{1}{c} [(\bar{\omega} \times \bar{R}_B) \times \bar{B}(\bar{R}_B)] \tag{30}$$

When the expression for V, equation (28) is used to evaluate V_{AB}, V_{CD} and $V_{CD'}$ and equations (23) and (24) are used to evaluate E_{AC} and $E_{AC'}$, a non-zero potential electric field perpendicular to $\bar{B}$ is obtained at point A. There is also a parallel component of the potential electric field at point A, this parallel component must satisfy the equation

$$\bar{E}_T \cdot \hat{B} = (-\frac{1}{c} \frac{\partial \bar{A}}{\partial t}) \cdot \hat{B} - \bar{E}_s \cdot \hat{B} = 0 \tag{31}$$

$\bar{E}_T$ is the total electric field at point A and $\bar{E}_s$ is the potential electric field of A ($\bar{E}_s$ has perpendicular components E_{AC} and $E_{AC'}$). Thus $\bar{E}_s$ has a parallel component given by

$$(\bar{E}_s)_{11} = \frac{1}{c} (\frac{\partial \bar{A}}{\partial t})_{11} \tag{32}$$

The total electric field (in the inertial frame, $\bar{E}_T$) is then given by

$$\bar{E}_T = \bar{E}_s - \frac{1}{c} \frac{\partial \bar{A}}{\partial t} \tag{33}$$

where E_s is made up of the parallel component $(1/c \cdot \partial\bar{A}/\partial t)_{11}$ and perpendicular components E_{AC} and $E_{AC'}$ and $\partial A/\partial t$ is given by equation (27). To convert to a frame moving with a satellite, one must add the field $1/c\ (\bar{V}_s \times \bar{B})$ where $\bar{V}_s = \bar{\omega} \times \bar{R}_A$ if the satellite corotates with the earth. Thus the electric field in the frame of a moving satellite, $(\bar{E}_T)_{rot}$, is given by

$$(\bar{E}_T)_{rot} = \bar{E}_T + \frac{1}{c}(\bar{V}_s \times \bar{B}) = \bar{E}_s - \frac{1}{c}\frac{\partial \bar{A}}{\partial t} + \frac{1}{c}(\bar{V}_s \times \bar{B}) \qquad (34)$$

when this expression was evaluated using the earth's internal dipole only and the Hones Bergeson boundary condition, the electric field was found to be zero in the frame of a satellite corotating (synchronous) with the earth.

$$(\bar{E}_T)_{syn} = 0 \qquad (35)$$

This is the expected result. The electric field as seen by an observer rotating with the conducting magnetized sphere (when the field lines are conducting and $\bar{E} \cdot \hat{B} = 0$) is everywhere zero. This zero result provides an important check on our computer program. Essentially, it states that starting with a boundary field (in the inertial frame) of $1/c \cdot \partial\bar{A}/\partial t - 1/c\ (\bar{V} \times \bar{B})$ in the presence of the $\partial\bar{A}/\partial t$ from the internal source only results in a zero total electric field in the frame of a corotating observer. This fact was later used to simplify the calculations when the field from an external $\partial\bar{A}/\partial t$ is included.

The Magnetospheric Electric Field from External Sources

We will now discuss a procedure that will allow us to map an ionospheric electric field seen by an observer rotating with the earth to an arbitrary satellite in the presence of an external $\partial\bar{A}/\partial t$.

To correctly proceed with the mapping procedure, the potential electric field in the ionosphere must be known in the inertial frame. We are given that the total electric field in the ionosphere in the rotating frame, $(\bar{E}_T)_{rot}$, is known. The electric field in the inertial frame $(\bar{E}_T)_{rest}$ is given by

$$(\bar{E}_T)_{rest} = (\bar{E}_{pot})_{rest} - \frac{1}{c}\left(\frac{\partial\bar{A}}{\partial t}\right)_{rest} \tag{36}$$

$$(\bar{E}_T)_{rot} = (\bar{E}_T)_{rest} + \frac{1}{c}(\bar{V} \times \bar{B}) \tag{37}$$

Thus
$$(\bar{E}_T)_{rot} - \frac{1}{c}(\bar{V} \times \bar{B}) = (\bar{E}_{pot})_{rest} - \frac{1}{c}\left(\frac{\partial\bar{A}}{\partial t}\right)_{rest} \tag{38}$$

$$(\bar{E}_{pot})_{rest} = (\bar{E}_T)_{rot} + \frac{1}{c}\left(\frac{\partial\bar{A}}{\partial t}\right)_{rest} - \frac{1}{c}(\bar{V} \times \bar{B}) \tag{39}$$

but $(\partial\bar{A}/\partial t)_{rest}$ is made up of two sources, the wobble of the internal dipole $(\partial\bar{A}/\partial t \text{ dipole})_{rest}$ and the external source $(\partial\bar{A}/\partial t \text{ external})_{rest}$. Similarly, $\bar{B}$ is made up of $\bar{B}_{dipole}$ and $\bar{B}_{external}$.

Thus $$\left(\frac{\partial \bar{A}}{\partial t}\right)_{rest} = \left(\frac{\partial \bar{A}}{\partial t}\ \text{dipole}\right)_{rest} + \left(\frac{\partial \bar{A}}{\partial t}\ \text{external}\right)_{rest} \tag{40}$$

$$\bar{B} = \bar{B}_{dipole} + \bar{B}_{external}$$

$$\left(\bar{E}_{pot}\right)_{rest} = \left(\bar{E}_T\right)_{rot} + \frac{1}{c}\left(\frac{\partial \bar{A}}{\partial t}\ \text{external}\right)_{rest} - \frac{1}{c}\left(\bar{V} \times \bar{B}_{external}\right) \tag{41}$$

$$+ \left[\frac{1}{c}\left(\frac{\partial \bar{A}}{\partial t}\ \text{dipole}\right)_{rest} - \frac{1}{c}\left(\bar{V} \times \bar{B}\right)_{dipole}\right]$$

The term in brackets on the right side of the equation is simply the Hones Bergeson term and in the case of a corotating satellite, this term adds up to a net zero contribution in the frame of the corotating satellite. We thus define $\left(\bar{E}_{pot}\right)_{rest}$ such that

$$\left(\bar{E}_{pot}\right)_{rest} = \left(\bar{E}_{pot}\right)_{rest} - \left[\frac{1}{c}\left(\frac{\partial \bar{A}}{\partial t}\ \text{dipole}\right) - \frac{1}{c}\left(\bar{V} \times \bar{B}\right)_{dipole}\right] \tag{42}$$

$$= \left(\bar{E}_T\right)_{rot} + \frac{1}{c}\left(\frac{\partial \bar{A}}{\partial t}\ \text{external}\right) - \frac{1}{c}\left(\bar{V} \times \bar{B}_{external}\right)$$

The complete solution to the problem evaluates the potential electric field $\left(\bar{E}_s\right)_{rest}$ at the satellite by evaluating the integral in equation (8) in the rest frame using $\left(\bar{E}_{pot}\right)_{rest}$, the potential electric field in the ionosphere in the rest frame. The integral is evaluated using the $\partial\bar{A}/\partial t$ from both the internal (dipole) and external sources. To the scalar potential

electric field determined in the inertial frame at the satellite is added the $\partial\bar{A}/\partial t$ from both the internal (dipole) and external sources, using equation (33). The $1/c\ (\bar{V} \times \bar{B})$ rotation field (external and internal $\bar{B}$) is then added to obtain the electric field in the reference frame of the satellite.

If the satellite is corotating with the earth, a simplification in this procedure can be used. It was shown above that the total electric field in a corotating reference frame is zero if one starts with an ionospheric boundary condition of

$$\frac{1}{c}\left(\frac{\partial\bar{A}}{\partial t}\right)\text{internal} - \frac{1}{c}\left(\bar{V} \times \bar{B}\right)\text{internal} \qquad (43)$$

in the inertial frame and evaluates the potential electric field at the corotation point using equation (8) when $\partial\bar{A}/\partial t$ is due to the internal source only. Then adds $\partial\bar{A}/\partial t$ from the internal source and finally adds in $1/c\ (\bar{V} \times \bar{B})$ to transform to the corotating reference frame.

Thus, if all of these steps (using the internal sources) are subtracted, the result should not change.

The shortened procedure which leaves out all of the internal terms, and which can be used in the case of a corotating satellite, is as follows:

1. Given a measurement of the total electric field in the ionosphere by an observer fixed on the earth, $(\bar{E}_T)_{rot}$, we define a

$$(\bar{E}_{pot})_{rest} = (\bar{E}_{pot})_{rot} + \frac{1}{c} \left(\frac{\partial \bar{A}}{\partial t}\right)_{external} - \frac{1}{c} (\bar{V} \times \bar{B}_{external})$$

2. Evaluate the integral and solve for the potential electric field at the satellite location using only the $\partial \bar{A}(r)/\partial t_{external}$ and the $(\bar{E}_{pot})_{rest}$ as the boundary condition.

3. Add in the external induction electric field at the satellite, $(\partial \bar{A}(r)/\partial t)_{external}$, and add in the corotation field $(1/c\ \bar{V} \times \bar{B}_{external})$ due to the external sources.

The result is the total electric field at the satellite in the frame of the rotating satellite, given a total ionospheric electric field, $(\bar{E}_T)_{rot}$, measured by an earth-based observer.

When this abreviated procedure (excluding the internal sources) is used with the computer program developed to calculate for the total electric field using the earth's dipole magnetic field with an arbitrary external $\partial \bar{A}/\partial t$, it yields identical results to those when all of the internal sources are included.

Section 5

PUBLICATIONS AND PRESENTATION

The following is the list of our publications and presentations which have resulted from worn on Contract No. N00014-80-C-0796 during the past year.

Publications

A Dynamic Model of the Magnetospheric Magnetic and Electric Fields for July 29, 1977 (W. P. Olson and K.A. Pfitzer). J. Geophys. Res., Vol. 87, No. A8, pp. 5943-5948, August 1, 9182.

The Entry of Magnetosheath Plasma as a Source of Steady State Magnetospheric Features, W. P. Olson and K. A. Pfitzer, submitted for publication in the Journal of Geophysical Research, May 1983.

Introduction to the Topology of Magnetospheric Current Systems. Presented at the Chapman Conference on Magnetospheric Currents, Irvington, VA, April 1983. McDonnell Douglas Astronautics Paper G8953. To be published in the Geophysical Monograph Series, Vol. 26, 1983.

Presentations

A Dynamic Magnetic Field Model (with K. A. Pfitzer). Presented at the 1982 Spring Meeting in Philadelphia, PA, May, 1982. McDonnell Douglas Astronautics Paper G8883-I.

Magnetospheric Configuration and Energetic Particle Effects Assoiciated with the SSC on 22 March 1979: CDAW-6 (with B. Wilken, D. N. Baker, T. A. Fritz, and K. A. Pfitzer). EOS, Vol. 63, No. 45, November 1982.

The Entry of Low Energy Plasma into the Magnetosphere and its Effects on Fields and Currents (with K. A. Pfitzer). Presented at the Chapman Conference on Magnetospheric Currents, Irvington, VA, April 1983. McDonnell Douglas Astronautics Paper G8952.

The Quantitative Representation of the Magnetospheric Electromagnetic Field for Specific Events (with S. Schneider and K. A. Pfitzer). To be presented at the 1983 Spring Meeting of AGU in Baltimore, Md.

The Induced Electric Field for Specific Magnetospheric Events (with K. A. Pfitzer). To be presented at the 1983 Spring Meeting of AGU in Baltimore, Md. McDonnell Douglas Astronautics paper No. G8973-I.

The Consequences of Low Energy Particle Entry into a Magnetically Closed Magnetosphere (with K. A. Pfitzer). To be presented at the 1983 Spring Meeting of AGU in Baltimore, Md. McDonnell Douglas Astronautics paper No. G8972-I.

The Induced Electric Field During the CDAW Events (with K. A. Pfitzer). To be presented at the IAGA/IUGG XVIII General Assembly in Hamburg, Germany, August 1983. McDonnell Douglas Astronautics paper No. G8978-I.

Low Energy Particle Entry into a Magnetically Closed Magnetosphere. To be presented at the IAGA/IUGG XVIII General Assembly in Hamburg, Germany, August 1983. McDonnell Douglas Astronautics paper No. G8979-I.

Quantitative Modeling of the disturbed Magnetospheric Magnetic Field (with K. A. Pfitzer). To be presented at the IAGA/IUGG XVIII General Assembly in Hamburg, Germany, August 1983. McDonnell Douglas ASstronautics paper No. G8980-I.

Quantitative Modeling of Induced Magnetospheric Fields and Plasma Response. To be presented at the IAGA/IUGG XVIII General Assembly in Hamburg, Germany, August 1983. McDonnell Douglas Astronautics paper No. G8981-I.

END

FILMED

7-83

DTIC